



# New chronology of the best developed loess/paleosol sequence of Hungary capturing the past 1.1 ma: Implications for correlation and proposed pan-Eurasian stratigraphic schemes

P. Sümegei <sup>a, b</sup>, S. Gulyás <sup>a, \*</sup>, D. Molnár <sup>a</sup>, B.P. Sümegei <sup>a, j</sup>, P.C. Almond <sup>c</sup>, J. Vandenberghe <sup>d</sup>, L. Zhou <sup>e</sup>, E. Pál-Molnár <sup>f</sup>, T. Töröcsik <sup>a, j</sup>, Q. Hao <sup>g</sup>, I. Smalley <sup>h</sup>, M. Molnár <sup>i, j</sup>, I. Marsi <sup>k</sup>

<sup>a</sup> University of Szeged, Department of Geology and Paleontology, Szeged, Hungary

<sup>b</sup> Institute of Archeology, Hungarian Academy of Science, Budapest, Hungary

<sup>c</sup> Lincoln University, Lincoln, Northern Canterbury, New Zealand

<sup>d</sup> Vrije Universiteit Amsterdam, Institute of Earth Sciences, the Netherlands

<sup>e</sup> University of Beijing, Department of Geomorphology and Quaternary Geology, China

<sup>f</sup> University of Szeged, Department of Mineralogy, Petrology and Geochemistry, Szeged, Hungary

<sup>g</sup> Institute of Geology and Geophysics, Chinese Academy of Sciences, Beijing, China

<sup>h</sup> University of Leicester, Department of Geography, UK

<sup>i</sup> Institute of Nuclear Research, Hertelendi Laboratory of Environmental Sciences, Debrecen, Hungary

<sup>j</sup> ICER Center, Institute of Nuclear Research, Hungarian Academy of Sciences, Debrecen, Hungary

<sup>k</sup> Hungarian Geological and Geophysical Institute, Budapest, Hungary

## ARTICLE INFO

### Article history:

Received 23 April 2017

Received in revised form

6 April 2018

Accepted 16 April 2018

Available online 18 May 2018

### Keywords:

Loess/paleosol sequences

Danubian basin

Revised chronology

New pan-Eurasian regional correlation

scheme

Middle and upper pleistocene

## ABSTRACT

In this paper, we are presenting a revised chronology of the best developed, longest (100 m) LPS in Hungary dating back 1.1 Ma: borehole Udvari-2A. It is based on a non-tuned age-depth model, built on the position of the Matuyama-Brunhes Boundary, Jaramillo and Olduvai Subchrons. Furthermore, on the assignment of formerly recorded uninterpreted geomagnetic reversals in both chrons. Other chronometric tools (AMS <sup>14</sup>C dating, biostratigraphy, tephrostratigraphy) yielding absolute ages and/or ensuring validation of these were also used. Records of a Middle Pleistocene gastropod index fossil *Neostyriaca corynodes* (400–140 ka) facilitated verification of ages between MIS 10 and MIS 6. Multiple age control points at 15, 25, 27, 45, 120, 191, 362, 430, 670, 780, 900, 990, 1070 ka were established for the last ca. 1.1 Ma. The resulting chronology is the best resolved independent one so far among Danubian Basin LPSs. In light of our data, the S3–S4 units were fused as S3 in all Serbian, and some Romanian sites and re-correlated with MIS 9. The results also point to a misassignment of the S5 units at these sites to MIS 13–15 leading to erroneous conclusions regarding paleoclimatic conditions and cyclicity. In our new stratigraphic scheme, these S5 paleosols were taken to represent the S4 paleosol and re-correlated with MIS 11. Finally, an ideal stratigraphic column dating back 1.1 Ma for SW Hungary was constructed and correlated with the Chinese loess/paleosol sequence of Xifeng and the benthic oxygen isotope record down to MIS 31.

© 2018 Elsevier Ltd. All rights reserved.

## 1. Introduction

Predicting climate and environmental changes is one of the most significant challenges of current research in earth sciences (Barnett and Schlesinger, 1987; Broecker, 1987; Friedli et al., 1986; Neftel et al., 1988; Huggert, 1991; Imbrie et al., 1993; Wake, 2013).

Recent advancements in science and computer technology have enabled the modeling of paleoclimatic records for the past (Joussaume and Taylor, 1995; Holden et al., 2010; Braconnot et al., 2012; Kageyama et al., 2012). To understand and model climate-ecosystem relations on a scale of multiple glacials-interglacials, continuous, well-resolved non-orbitally tuned paleoclimatic records with a firm chronology are needed. While marine and ice core sequences provide us with a reference on climate variability on such scales (McManus et al., 1999; Lisiecki and Raymo, 2005;

\* Corresponding author.

E-mail address: [gulyas.sandor@geo.u-szeged.hu](mailto:gulyas.sandor@geo.u-szeged.hu) (S. Gulyás).

Raymo et al., 2006; Jouzel et al., 2007; Parrenin et al., 2007; de Vernal and Hillaire-Marcel, 2008; Loulergue et al., 2008; Lüthi et al., 2008; Lang and Wolff, 2011), terrestrial records with a precise chronology yield us information on how these changes translate to terrestrial ecosystems (Williams et al., 1997; Kashiwaya et al., 2001; Prokopenko et al., 2001, 2002; Tzedakis et al., 2006). Among terrestrial deposits loess/paleosol sequences are among the most common and prominent type of paleoarchives of Quaternary climate changes (An et al., 1990; Pécsi, 1990, 1993; Pye, 1995; Lu and An, 1998; Kemp, 2001; Porter, 2001, 2007). Besides China (Kukla, 1987; Liu et al., 1987, 1988; An, 2000; Lu et al., 2004; Hao and Guo, 2005; Hao et al., 2012), one of the most significant loess areas, which can help us understand the climatic evolution of the past 0.8–1 million years is found in the Middle and Lower Danube Basin. The antiquity of these plateau-positioned loess paleosol sequences (LPSs) is supported by magnetostratigraphic investigations complemented by other chronometric and stratigraphic tools (for a comprehensive review see Fitzsimmons et al., 2012; Marković et al., 2015). The well-known LPSs of Krems in Austria (Fink and Kukla, 1977; Hambach et al., 2008; Terhorst et al., 2014), Paks in Hungary (Pécsi and Pevzner, 1974; Márton, 1979; Pécsi, 1993; Sartori et al., 1999; Thiel et al., 2014; Újvári et al., 2014a), Batajnica (Marković et al., 2009), Mošorin (Marković et al., 2012a, 2015) and Stari Slankamen in Serbia (Marković et al., 2011, 2015; Murray et al., 2014) of the mid-Danube Basin all belong to this series (Fig. 1).

Similarly, the Lower Danube Basin profiles of Koriten (Jordanova and Petersen, 1999), Viatovo in Bulgaria (Jordanova et al., 2007, 2008), Mostista (Panaiotu et al., 2001), Mircea Voda (Bugge et al., 2009, 2013) and Zimnicea borehole in Romania (Rădan, 2012) may be mentioned. It is therefore no surprise the glacial-interglacial paradigm was founded on Danubian loess/paleosol sequences (DBLPSs) (Kukla, 1977, 1978). Marković et al. (2015) recently proposed a pan-European loess/paleosol stratigraphic system and a master chronology, which was considered as a sound basis for Northern Hemisphere correlation and climate cycle analysis (Kukla and Cilek, 1996; Kukla, 2005; Bugge et al., 2013; Marković et al., 2012a; b; 2015; Basarin et al., 2014).

In addition, some DBLPSs display strong similarities with those of the Chinese loess plateau in terms of paleomagnetic characteristics interpreted as an outcome of similar controls on deposition and magnetic susceptibility signal acquisition (Bronger, 2003; Marković et al., 2011, 2012a, 2015). An exception is perhaps the area of Southern Serbia (Obrecht et al., 2016). However, as noted in several studies, DBLPSs tend to be thinner compared to LPSs of the Chinese loess plateau (Marković et al., 2012a, 2015). A notable exception is perhaps the LPS of Tolna Hills, SW Hungary, where a borehole has recovered the thickest Quaternary sequence (98 m) in Hungary and the entire Carpathian Basin (Middle DBLPSs) (Kolozsár and Marsi, 2010a; b) (Fig. 1). Magnetostratigraphic results underline the antiquity of the LPS preserved at borehole Udvari-2A,

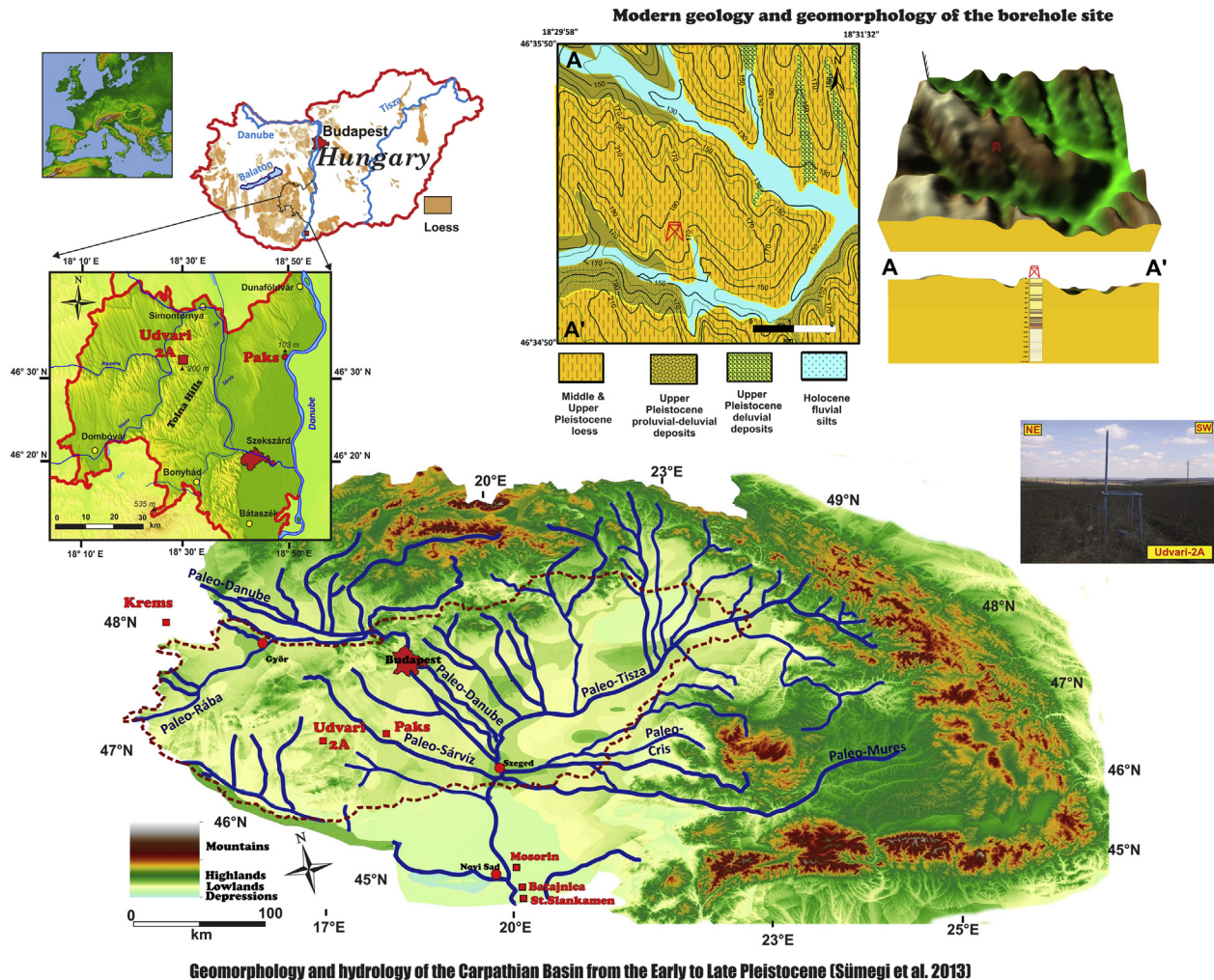


Fig. 1. Location, paleohydrology, modern morphology, geology of the study site.

which dates back as far as 1.1 Ma (Márton, 1998; Koloszar, 1997, 2003; Koloszar and Marsi, 1997; Koloszar and Lantos, 2001; Koloszar et al., 2001; Sümegei et al., 2011b). Initial chronostratigraphy was established via correlations of the magnetic polarity zones of the borehole (Márton, 1998) with the global polarity timescale of Richmond (1996). However, there is a major caveat regarding the accuracy of this initial chronostratigraphy we must emphasize. Although Márton (1998) recorded numerous reversed polarity zones within the Brunhes chron (C1n on Fig. 2), not one was chronologically interpreted apart from the Matuyama–Brunhes Boundary (MBB). In addition, borehole magnetic susceptibility measurements (Bucsi-Szabó et al., 1997) were wiggle matched with the marine curve of Crowhurst (2002) (Koloszar and Marsi, 2010a; b).

Although recent developments in pIRIRSL provide potential for securely attaining ages up to 300 ka (corresponding to MIS8) (Thiel et al., 2011, 2014; Li and Li, 2012; Vasiliniuc et al., 2012; Murray et al., 2014; Schmidt et al., 2014), in some cases even up to ~600 ka (corresponding to MIS15) (Roberts, 2012; Suangwen et al., 2012; Brown and Forman, 2012; Ankjaergaard et al., 2016; Chapot et al., 2016), in borehole Udvari 2A poor preservation due to unconsolidated nature of much of the core samples, as well as the lack of casing prevented us from retrieving samples appropriate for luminescence analysis trials.

Amino acid racemization stratigraphy has been reported to be similarly successful on various fossil gastropod taxa around the world (Oches and McCoy, 1995a; b; 2001). Application of this technique was warmly welcomed in Vojvodinian sites of the DBLPSs with promises of interprofile stratigraphic improvements.

On the basis of investigations done at Ruma and Stari Slankamen AAR chronology was considered to be able to securely define the last 4–5 interglacial cycles down to MIS 11, 13 (Marković et al., 2006, 2011; 2012a,b, 2015). However, in AAR results presented for Ruma and Stari Slankamen (Marković et al., 2006, 2011, 2015), the original remarks of Oches and McCoy (2001) do not seem to apply on loess beyond L2. Data for V-L5 is missing, ratios for VL-7 and VL-9 are almost the same (0.51 and 0.52, respectively) (Marković et al., 2011) rendering discrimination highly ambiguous. AAR chronology on its own thus can not yield independent absolute ages as two already available independent bracketing ages of the sampled unit are needed for calibration. Rather, based on available independent ages it can create a relative chronology, fidelity of which is also dependent on the chronostratigraphical assignment of the studied loess units beyond L3. So because of the mentioned disparities AAR was avoided in our work.

Without recourse to the dating techniques mentioned above, we have relied primarily on other chronometric tools like radiocarbon analysis, biostratigraphy and magnetostratigraphy for the establishment of independent absolute chronologies. Once ages verified by independent data are available, these are then used as fixed control points between which chronostratigraphy is built by simple interpolation. In some “ancient” Serbian profiles orbital tuning was adopted for constructing chronostratigraphy to find orbital cycles in the data (Markovic et al., 2012b; Basarin et al., 2014) Such records are however not useful for testing the astronomical theory once orbital tuning is employed, because the same was used to define the chronology (Rapp, 2012).

A revisit with the addition of new chronological, litho- and

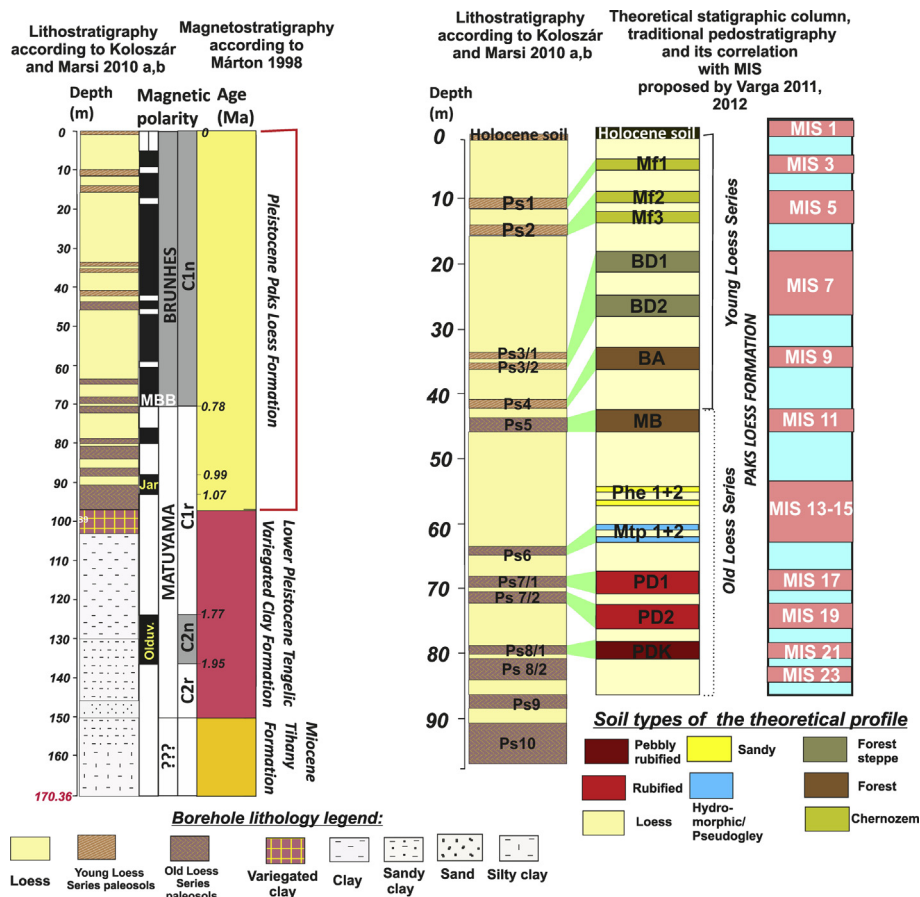


Fig. 2. Original magneto- (Márton, 1998) and lithostratigraphy of the studied borehole site as well as its original correlation with the Hungarian lithological and pedostratigraphical scheme (Koloszar and Marsi, 2010 a; b) using the example of recently proposed theoretical lithological and pedostratigraphical column of Varga (2011, 2012) for the area of Hungary.

biostratigraphical data, as well as the interpretation of uninterpreted polarity zones was thus highly desired to update and develop a new non-orbitally tuned chronostratigraphy of the longest regional paleoarchive of borehole Udvari-2A (Sümegi et al., 2011b). It is the cornerstone of future correlation with other regional and extraregional records, as well as the assessment of temporal variation of mass accumulation rates and paleoclimatic cycles. Availability of new marine (Lisiecki and Raymo, 2005) and terrestrial proxy reference records (Liu et al., 1987, 1988; Lu et al., 2004; Guo et al., 2009a; b; Sun et al., 2009; Wu and Wu, 2011; Zhou et al., 2014) as well as geomagnetic intensity timescales (Michalk et al., 2013; Singer et al., 2014) called for a revision as well.

## 2. Location, stratigraphy and modern climate of the site

The borehole Udvari-2A is located in the central plateau part of the Tolna Hills, SW Hungary (Fig. 1). The modern climate of the area is temperate (Köppen Bs) with strong oceanic (Köppen Cf) and sub-Mediterranean climatic influences (Supplementary Fig. 1). This is mainly seen in higher temperatures, multiple rainfall peaks and

elevated hours of sunshine compared to areas without sub-Mediterranean influences. The mean annual temperature is around 9–9.5 °C. The average annual precipitation of 650 mm may reach 700–750 mm in the western part of the region, including the location of the investigated borehole. While on the eastern side, where the well-known Paks brickyard site (Pécsi, 1993; Pécsi et al., 1995; Sartori et al., 1999; Újvári et al., 2014a) is located it's slightly below 650 mm (Ádám et al., 1981; Hungarian Meteorological Survey). Yet rainfall is still higher compared to the more southern Vojvodina LPS sites of Stari Slankamen, Mošorin or Batajnica (Marković et al., 2009, 2011, 2012a, 2015). According paleoecological data, these climatic influences were present in the area from 400 ka onwards (Sümegi et al., 2012a; b) and must have influenced soil formation.

The borehole, drilled in the 1990s using a rotary stage coring system yielding cores of 10 cm in diameter, starts from an elevation of 178 m ASL in a clear plateau position and penetrates 170.3 m. It exposes a series of 150 m Quaternary sediments overlying Miocene Lake Pannon deposits (Fig. 2). The upper 97 m represents the Paks Loess Formation (Koloszár, 1997, 2003; Koloszár and Marsi, 2010a,

**Table 1**

The theoretical pedostratigraphic column of the past 1 My for Hungary with paleosols used in the Hungarian Quaternary Stratigraphic Pedostratigraphic Scheme.

Absolute Age	International Geomagnetic Polarity Scale	Lithostratigraphy	Theoretical Quaternary Stratigraphy and Pedostratigraphy (Varga, 2011; Újvári et al., 2014a)	Pedological character after Bronger (2003) in Varga (2011), Újvári et al. (2014a), Horváth and Bradák (2014)	Site of original description after Pécsi et al. (1995)	Designation in system of Markovic et al. (2015) proposed by this study	Theoretical correlation with marine oxygen isotope record of Lisiecki and Raymo (2005) according to Varga (2011), Újvári et al., 2014a)
0	BRUNHES	Paks Loess Formation	Holocene soil Mf1 (Mende Felső 1 = Mende Upper 1) paleosol Mf2 (Mende Felső 2 = Mende Upper 2) paleosol Mf3 (Mende Felső 3 = Mende Upper 3) paleosol Bd1 (Basaharc Dupla 1 = Basaharc Double 1) paleosol Bd1 (Basaharc Dupla 2 = Basaharc Double 2) paleosol BA (Basaharc Alsó = Basaharc Lower) paleosol MB (Mende Bázis = Mende Base) paleosol Phe 1 (Paks Homokos = Paks sandy forest) paleosol Phe 2 (Paks Homokos = Paks sandy forest) paleosol Mtp 1 (Mende-tápiósüly = Mende-tápiósüly) paleosol Mtp 1 (Mende-tápiósüly = Mende-tápiósüly) paleosol	– chernozem-serozem  chernozem  chernozem  chernozem  chernozem  brown forest soil  brown forest soil  sandy and brown forest soil  sandy and brown forest soil  hydromorphic soil, pseudogley*  hydromorphic soil, pseudogley*	– Mende  Mende  Mende  Basaharc  Basaharc  Basaharc  Mende  Paks  Paks  Mende-Tápiósüly  Mende-Tápiósüly	H-S0 H-L1S1  H-S1  H-S1  H-S2  H-S3  H-S4  H-S5S1  H-S5S2  H-S5S3  H-S5S4	MIS 1 MIS 3  MIS 5  MIS 7  MIS 9  MIS 11 MIS 13  MIS 15
780	MAT		PD1 (Paks Dupla 1 = Paks Double 1) paleosol PD2 (Paks Dupla 2 = Paks Double 1) paleosol PDK (Paks-Dunakömlöd) paleosol Pv1 Pv2 Pv3	rubified brown forest soil rubified brown forest soil rubified brown forest soil basal red soils/red clays	Paks  Paks  Paks, Dunakömlöd	H-S6 H-S7 H-S8 HS9-10-11	Mis 17 MIS 19 MIS21 MIS 23-
1000 1200 –3600		Tengelic Red Clay Formation	Tengelic Clay	variegated red clay complex	SW Hungary	H-S12	?

b.) according to the accepted Hungarian Quaternary Stratigraphic and Pedostratigraphic Scheme (HQSPS) (Table 1) (Pécsi, 1975, 1993; Pécsi et al., 1995; Sartori et al., 1999; Varga, 2011, 2012; Horváth and Bradák, 2014; Újvári et al., 2014a). Koloszár (1997) and Koloszár and Marsi, (2010a,b) originally describes 13 paleosol units (marked as Ps1–Ps10) in the upper 97 m (Fig. 2). Some of them were determined as double paleosols (e.g. Ps3, Ps7 and Ps8). The original lithostratigraphy presented on Fig. 2 was developed using visual identification of the main stratigraphic units in the core (Koloszár, 1997; Koloszár and Marsi, 2010a; b), but was heavily influenced by the recognized reference units of the HQSPS (Table 1.) (Pécsi, 1975, 1993; Pécsi et al., 1995; Sartori et al., 1999; Varga, 2011, 2012; Horváth and Bradák, 2014; Újvári et al., 2014a; Marković et al., 2015). In this stratigraphy, the lowermost loess-paleosol packages (LPPs) of the Paks Loess Formation covering an age between ca. 1 Ma and 400 ka (MIS 27–11) have been described as “Old Loess”, and the overlying LPPs as “Young Loess” (Fig. 2). The boundary between the two was based on shift in the general pedological features of older paleosols (Pécsi, 1979, 1990; 1993; Pécsi and Schweitzer, 1993; Fitzsimmons et al., 2012).

The intercalated paleosols were originally described by assigning them to the zonal paleosol system of HQSPS (Pécsi, 1975; Pécsi et al., 1995; Koloszár, 1997; Koloszár and Marsi, 2010a; b) (Table 1). The lowermost paleosols were described as Mediterranean rubified paleosols (Ps10–Ps7) (Fig. 2) overlain by brown forest type paleosols (Ps6–5) representing the so-called “Old Loess Series”. Loess layers above Ps6 have been noted to present some hydromorphological features interpreted to represent infusion or water-influenced loess deposits (Koloszár, 1997; Koloszár and Marsi, 2010a; b). The uppermost four paleosols corresponding to the “Young Loess Series” were determined as forest steppe (Ps4–Ps2), as well as chernozem type soils (Ps 1). A later proposal of a theoretical stratigraphic column based on the HQSPS (Varga, 2011, 2012) with assumed correlations to the record of Lisiecki and Raymo (2005) depicted on Fig. 2 was used to help visualize this original pedostratigraphic and chronostratigraphic correlation of the studied borehole system. Koloszár and Marsi (2010a; b) presented a correlation of their MS curve from measurements done by Bucsi-Szabó et al. (1997) with the marine curve of Crowhurst (2002). According to their correlation, the first paleosol (Ps1) corresponds to MIS 3, the second (Ps2) to MIS5, the third double paleosol (Ps3/1 and Ps 3/2) to MIS7, the fourth (Ps 4) to MIS 9, the fifth (Ps5) to MIS 11, the sixth (Ps 6) to MIS 15 (Fig. 2). While the first member of the 7th double paleosol (Ps7/1) was correlated to MIS 17, the second (Ps7/2) to MIS 19. The double paleosol Ps 8/1 and Ps 8/2 were considered to represent MIS 21 (Fig. 2). The lowermost paleosols Ps9 and Ps10 was correlated with MIS 23–25 and 27–30, respectively. No visual signs of soil erosion, mixed loess layers or fluvial sandy intercalations have been documented in the core sequence. Presence of minor hiatuses representing short-periods of non-deposition can also be fully excluded as these represent so-called debunked soil forming intervals when paleosols form as an interaction of slow deposition and climatic influences. In contrast, the nearby ca. 45 m-long sequence of Paks, approximately 35 kms to the east, is by no means undisturbed and complete. Numerous erosional hiatuses have been documented in its upper parts. These hiatuses were interpreted to represent hillslope erosions, so-called dells in Hungarian geography by Pécsi (1975), Pécsi et al. (1995) and others (Frechen et al., 1997; Sartori, 2000; Thiel et al., 2014; Újvári et al., 2014a). The total thickness of this latter LPS, covering roughly the same time-period as our record, is about half of our profile. It must be noted that our site is found in a clear plateau position today. It was in a similar position far from creeks and river courses from the Early Pleistocene onwards as seen on the paleohydrological map of Fig. 1. Conversely, the site of Paks occupies a small depression closer to

the modern Danube. Rendering it more prone to past downslope erosion and soil transport. It was also closer to the Paleo-Sárviž creek (Fig. 1) from the Early Pleistocene till about 20 ka when the Danube occupied its modern position (Sümegei et al., 2012a; b).

### 3. Material and methods

The core was resampled in 2008 at 25 cm increments to attain data for higher resolution multiproxy analysis to be presented elsewhere (Sümegei et al., 2011b). The poor preservation and unconsolidated nature of some parts hampered shorter interval sampling. A visual re-evaluation of the samples enabled us to present a revised lithostratigraphy. Dry color was determined using the Munsell color scale. To avoid potential future confusions, litho- and pedostratigraphic designation of the identified loess-paleosol units were done independently of the HQSPS and theoretical stratigraphic column presented on Fig. 2. Instead, the Chinese stratigraphic nomenclature (Liu et al., 1985; Kukla and An, 1989), also adopted in Serbia (Marković et al., 2008, 2009, 2011, 2015) and at some Hungarian sites too (Sümegei et al., 2011a; b; 2015), was used for the lithostratigraphic description. Names were derived from the letters of the borehole U2 with the designation S corresponding to paleosols and L to loess units (U2-S0 U2L1 etc.). In this system loess and paleosols appear with increasing numbering corresponding to older ages. Thus, S0 represents the modern soil, L1 the last glacial loess, and S1 the last interglacial paleosol. Pedostratigraphic nomenclature followed the USDA system of soil taxonomy (USDA, 1992). An interpretation of the previously unassigned magnetic polarity zones (Márton, 1998; Koloszár and Marsi, 2010a; b) complemented by new radiocarbon ages from the uppermost 5 m of the profile have been used as means to derive a revised chronostratigraphy. In addition, the occurrences of an important faunal element chronostratigraphic marker restricted to the cold periods of Middle Pleistocene have also been considered for bracketing interglacial paleosols. Finally, the stratigraphy was correlated to other long LPSs on the basis of the chronology supplemented with MS data. Magnetic susceptibilities as a promising tool for interprofile correlation are reliable only with independent age control. So, using the characteristic MS pattern as a stratigraphic tool along with the newly established chronology, litho- and pedostratigraphy, our records were correlated with the regional records of similar age in Hungary (Paks) (Pécsi, 1995; Frechen et al., 1997; Sartori, 2000; Thiel et al., 2014; Újvári et al., 2014a), Serbia (Stari Slankamen, Batajnica, Mošorin, Ruma) (Marković et al., 2006, 2009, 2011, 2015), Bulgaria (Koriten, Viatovo) (Jordanova and Petersen, 1999; Jordanova et al., 2007, 2008) Romania (Mostistea, Mircea Voda, Zimnicea) (Panaiotu et al., 2001; Buggle et al., 2009, 2013; Rădan, 2012). In addition, cross-correlation was attempted with other long-known and studied Chinese LPS of Xifeng (Liu et al., 1987, 1988; Lu et al., 2004; Guo et al., 2009a; b; Sun et al., 2009; Wu and Wu, 2011; Zhang et al., 2015) using a synthesis stratigraphical column based on the U2-A borehole sequence.

#### 3.1. Magnetostratigraphy and magnetic susceptibility

Results of magnetic polarity measurements carried out formerly in the laboratory of the Hungarian Geological Institute and published in an interim report were adopted in our work (Márton, 1998). Within the Matuyama reversed chron (C1r in Fig. 2) 3 normal polarity zones were recorded, but only two were chronologically interpreted (Márton, 1998). It is important to note some potential caveats of the interpretation of polarity zones in our borehole record. First, measurements were not continuous. In

addition, as core samples were taken much later than the on-site stratigraphic description sampling was somewhat biased. Either one meter increments and/or major visually identified stratigraphic units of Koloszár (1997) were used as a target. Due to this lower resolution in sampling for paleomag investigations (Márton, 1998) compared to global records used for establishing the global paleomag intensity timescale (e.g. Singer, 2014; Singer et al., 2014), some of the excursions might have been missed. So, other tools from biostratigraphy and intercorrelation with age-controlled pedostratigraphic and lithostratigraphic units of regional and extraregional records had to be adopted for crossvalidation.

Magnetic susceptibility was recorded on the newly taken (in 2008) core samples using a Bartington MS2 system at the University of Szeged Department of Geology and Paleontology (USZ-DGP) (frequency 2.7 kHz) (Sümeği et al., 2011b). Prior to the start of the measurement, all samples were crushed in a glass mortar. Then samples were cased in plastic vials and dried in air in an oven at 40 C for 24 h. Afterwards, samples were weighed and magnetic susceptibilities were recorded six times and the average values of weight corrected mass-specific susceptibility were computed and reported.

Complex univariate and multivariate statistical evaluation of magnetic susceptibility values was implemented aiding stratigraphic interpretations (Davies, 2002). A cluster analysis of the magnetic susceptibility values using the UPGMA algorithm and the Minkowski similarity distance metric – it reduces within group variances while increasing intergroup variances – was also implemented to identify groups of similar character in terms of ferromagnetic mineral formation. The formerly unidentified polarity zones were determined. These new and previously interpreted paleomagnetic excursions were recorelated with the global geomagnetic polarity timescale (GITS) presented in Michalk et al. (2013) and Singer et al. (2014) compiled from their and other authors' datasets (Langereis et al., 1997.; Nowaczyk and Frederichs, 1999; Nowaczyk and Knies, 2000; Lund et al., 2001, 2006.; Singer, 2007, 2014; Singer et al., 2002, 2008a, 2008b, 2014). In addition, the paleomagnetic record of the latest INQUA 2016 Global chronostratigraphical correlation table for the past 2.7 ma was used as well (Cohen and Gibbard, 2016).

### 3.2. Radiocarbon dating

As the upper 0.85 m corresponded to the modern soil, gastropod samples submitted to AMS <sup>14</sup>C dating were confined to the depths between 1.25 and 4 m. Certain herbivorous gastropods are known to yield reliable ages for dating deposits of the past 50 ka with minimal error on the scale of perhaps a couple hundred years (Hertelendi et al., 1992; Sümeği and Hertelendi, 1998; Pigati et al., 2004, 2010; 2013; Sümeği et al., 2007; Xu et al., 2011; Újvári et al., 2014b). Our taxa were chosen accordingly. For the analysis, shells of *Chondrula tridens* (MÜLLER 1774), *Granaria frumentum* (DRAPARNAUD, 1801) and *Fruticicola fruticum* (MÜLLER 1774) were used. They are of similar size ranges having similar habitat and feeding preferences. Shells were ultrasonically washed and dried at room temperature. Surficial contaminations and carbonate coatings were removed by pretreatment with weak acid etching (2% HCL) before graphitization (Sümeği and Hertelendi, 1998). Measurements were done in the internationally referenced AMS laboratory of Seattle, WA, USA. Conventional radiocarbon ages were converted to calendar ages using the software Oxcal 4.2 online (Bronk Ramsey, 2009) and the most recent Intcal13 calibration curve (Reimer et al., 2013). Calibrated ages are reported as age ranges and mean age at the 2-sigma confidence level (95.4%).

### 3.3. Occurrences of a chronostratigraphic index fossil of the cold periods of the Middle Pleistocene

The Alpine *Neostyriaca* genus is represented by two taxa in the modern European gastropod fauna: *Neostyriaca strobili* (STROBEL, 1850) and *Neostyriaca corynodes* (HELD, 1836). *Neostyriaca corynodes* is a clear cold-loving mollusk with modern distribution areas in the Alps and its' northern foothill areas Supplementary Fig. 2. It is well-recorded in the Pleistocene deposits of Europe as well (Klemm, 1969). In Hungary *Neostyriaca corynodes* was noted in Middle Pleistocene deposits from the 1960s onwards (Krolopp, 1961, 1970, 1973, 1977, 1981, 1994; Kretzoi and Krolopp, 1972; Kaiser et al., 1998; Hum and Sümeği, 2000, 2001; Hum, 2002, 2005, 2007). It is an important index fossil of the younger part of Middle Pleistocene loess deposits of the Carpathian Basin. It generally turns up with other cold-loving steppe elements in periods characterized by strong coolings of the later glacials of the Middle Pleistocene. But a mixed appearance of the taxon with xerothermophilous and mesophilous elements above well-observed paleosols has been noted in several sections of SE Transdanubia (Hum and Sümeği, 2000, 2001; Hum, 2002, 2005, 2007) as well. It was interpreted as marking the transition to the next cool climatic phase. The taxon appeared in the Carpathian Basin between 400 and 140 ka (Krolopp, 1961, 1970, 1973, 1977, 1981, 1994; Kretzoi and Krolopp, 1972; Kaiser et al., 1998; Hum and Sümeği, 2000, 2001; Hum, 2002, 2005, 2007). Not a single stratigraphic work is known to have mentioned glacials older than 400ka as yielding representatives of the referred taxon from loess or freshwater deposits (Krolopp, 1961, 1970; 1973, 1977; 1981, 1994; Kretzoi and Krolopp, 1972; Brunnacker et al., 1980; Kaiser et al., 1998; Hum and Sümeği, 2000, 2001; Hum, 2002, 2005; 2007; Pazonyi et al., 2014). The first appearance is dated between 400 and 300 ka, found in the *Helicigona vertesi* biozone (MIS 10) at the site of Vértesszőlös (Krolopp, 1973, 1977, 1981, 1994). The MIS 10 presence of *Neostyriaca corynodes* is justified by other data from Hungary as well. In some SE Transdanubian sites the presence of this taxon was recorded both below and above a well-developed paleosol horizon (BA= Basaharc Lower see Table 1), whose age can be independently confined. An important tephra marker horizon (Bag Tephra) was recorded below the BA paleosol at several SE Transdanubian sites. In addition, in some sites the tephra horizon occurred together with the biostratigraphic marker gastropod *Neostyriaca corynodes* (Hum and Sümeği, 2000, 2001; Hum, 2002, 2005, 2007). A similar coincidence of a tephra and *Neostyriaca corynodes* was also recorded at the northern Hungarian site of Basaharc right below the BA paleosol horizon (Sümeği, 1991; Krolopp, 2005, 2006; Sümeği and Sümeği et al., 2011a). The Bag Tephra is considered as a widespread chronological marker recorded at 12 Hungarian sites between the BA (Basaharc Lower) and MB (Mende Base see Table 1) paleosols (Kriván and Rózsavölgyi, 1964; Juvigné et al., 1991; Horváth et al., 1992; Pouclet et al., 1999; Hum and Sümeği, 2000, 2001; Horváth, 2001; Hum, 2007). It has been identified in one Slovakian site as well. Although it must be emphasized that its age is poorly constrained (between 360 and 380 and 788 ka) (Pouclet et al., 1999). Horváth (2001) placed the age of the tephra between MIS 8 and MIS 10. The exact age of 351 ka based on tephrostratigraphical correlation with the Villa Senni Tuff has been questioned (Sági et al., 2008). Correlation of the paleosols bracketing the tephra (BA and MB see Table 1 for nomenclature) with MIS 11 and MIS 9 was proposed by Oches and McCoy (1995a, b) on the basis of AAR results. The age of the BA paleosol was recently taken to most likely represent MIS 9 based on pIRIR290 measurements at Paks by Thiel et al. (2014). Field

observation of the Bag Tephra in the loess below this paleosol by Thiel et al. (2014) in their profile further corroborates the MIS 9 age of this paleosol.

The second appearance is dated between 180 and 140 ka (MIS 6) in general (Sümegei et al., 2002, 2011a; Sümegei and Krolopp, 2006; Sümegei, 2007). At some sites, a third intermediate appearance has also been reported between these two Middle Pleistocene intervals (Klemm, 1969; Hum and Sümegei, 2000, 2001; Hum, 2002, 2005; 2007; Krolopp, 2005). However, due to the general absence of well-resolved, independently dated MIS 8 layers containing this faunal element, the exact timing of this third appearance is tentative. Occurrences of this taxon in the studied profile helped us to confine the timescales of major loess units. In addition, as the presence of this taxon reliably brackets paleosol units, it was used to crosscheck and update the lithostratigraphy determined visually by Koloszár (2003), Koloszár and Marsi (2010a,b).

### 3.4. Age-depth modeling and MAR calculations

Finally based on the revised chronology, an age-depth model was constructed for the entire past 1.1 Mys via polynomial interpolation between new age-tiepoints. Sedimentation rates ( $SR = mm \cdot a^{-1}$ ), as well as mass accumulation rates ( $MAR = g \cdot m^{-2} / year$ ) have been calculated between the individual tiepoints for the entire sequence, and the upper  $^{14}C$  dated part separately, using a modified methodology presented in Tegen and Laci (1996), Kohfeld and Harrison (2000), Frechen et al. (2003).

## 4. Results

### 4.1. A revised litho-pedostratigraphy

After the 2008 resampling of the core sequence, a thorough visual reevaluation complemented later by biostratigraphic data presented in section 4.4 and magnetic susceptibility measurements enabled us to develop a revised litho-, pedostratigraphy of the LPS of Udvari-2A for the interval of 100 m. This has been later corroborated by geochemical data presented in Sümegei et al. (2011b). In the sequence 13 interglacial paleosols (U2-S1 to U2-S13) could have been identified (Fig. 3). The lowermost paleosol (U2-S1) developed on the underlying red clays of the Tengelic Clay Formation (Fig. 2). Below the modern soil (U2-S0), two weakly developed light yellowish-brown (10YR 6/4) paleosols (bBw1, bBw2) were identified at the depths of 3 and 4.5 m (U2-L1S1, U2-L1S2). The top of the first interglacial paleosol (MIS5) U2-S1 was located at the depth of 8–11 m composed of A, B horizons (b1A, b1B) of pale brown hue (10YR 6/3). These are underlain by a B2 horizon (b1B2) at a depth of 12–14 m under which a well-cemented carbonate layer was observed (b1B2kn). This pedological feature also confirms that the soils above are autochthonous (Bronger, 2003). The next weakly developed pedocomplex of U2-S2 found between 18 and 23.5 m is composed multiple embryonic soils (b2Bw1-b2Bw3) with light greyish brown hue (10Y 5/2). The pedocomplex of U2-S3 between the depths of 31.5 and 36 m has well developed greyish dark brown (2.5Y 4/2) Bw horizons (b3B, b3Bw) separated from the underlying B2 (b3B2) horizon by a zone of carbonate accumulation (b3Bkn).

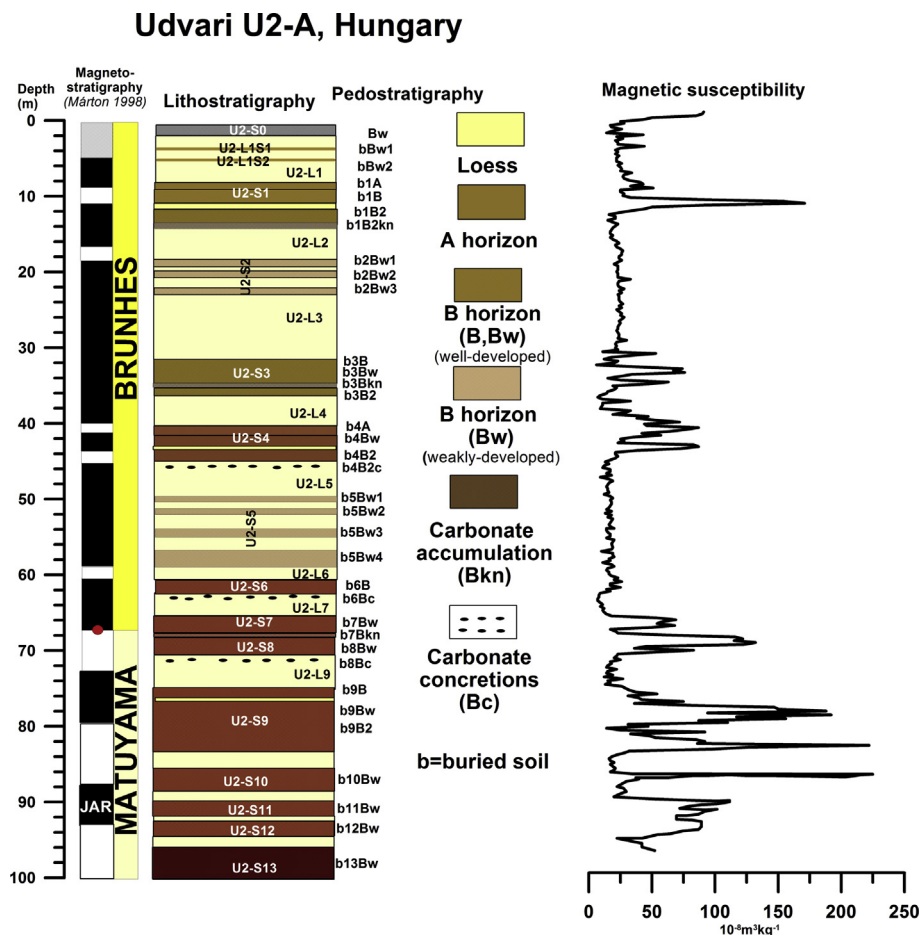


Fig. 3. A revised litho- and pedostratigraphy of the Udvari-2A borehole sequence and measured magnetic susceptibility values down to a depth of 100 m.

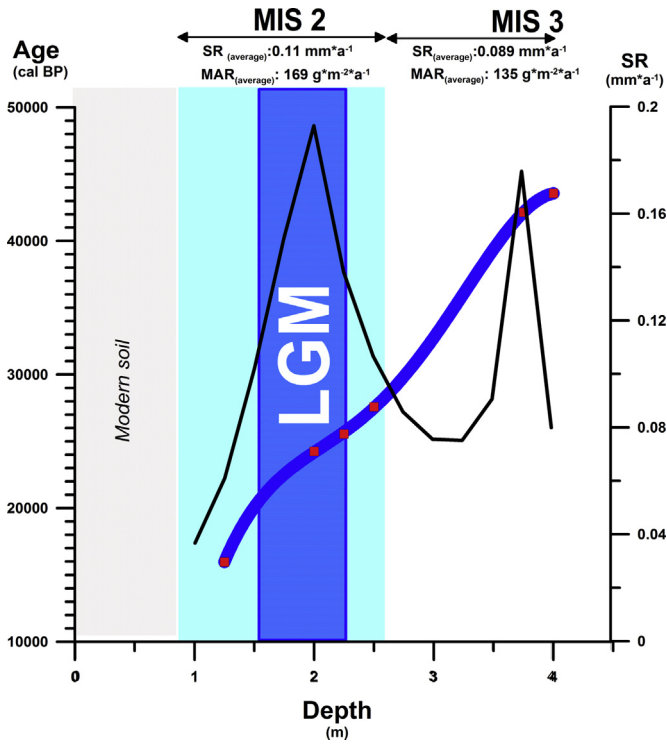


Fig. 4. Age-depth model for the upper 4 m of the borehole and calculated MARs.

Bkn horizons are resistant to soil erosion and present further evidence of autochthonous soil formation of the two membered pedocomplex (Bronger, 2003).

The U2-S4 pedocomplex between 40.5 and 45 m is made up of two well-developed dark brown (10YR 3/3) B horizons (b4Bw, b4B2) topped by a light brown A (2.5Y 6/3) (b4A) horizon. The pedocomplex is underlain by numerous carbonate concretions of cm size (b4B2c). As mentioned previously this pedological feature also confirms that the soils above are autochthonous (Bronger, 2003). The U2-S5 pedocomplex between the depths of 50 and 59 m is made up of several weakly developed soils (b5Bw1–b5Bw4). The upper ones have moderate clay and some sand content (b5Bw1, b5Bw2), while the lower (b5Bw3, b5Bw4) have higher clay content and display some hydromorphic characteristics. No signs indicating the presence of pseudogley was noted though. U2-S6 between the depth of 61–63 m has a well-developed reddish brown (5YR 5/3) B horizon (b6B) underlain by carbonate concretions of cm size (b6Bc).

The two paleosols (U2-S7, U2-S8) straddling the MBB are rubified (2.5/4) with well-developed compact B horizons (b7Bw, b8Bw) separated by a zone of carbonate accumulation (b7Bkn). Under the U2-S8 paleosol, a zone of carbonate concretions ranging between 1 and 8 cm in size was noted (b8Bc). The pedocomplex (U2-S9) between 76 m and 84 m is likewise rubified (2.5/4) with well-developed B horizons (b9B, b9B2 b9Bw). The paleosol U2-S10 between 86 and 88 m has a reddish-brown hue (2.5YR 3/4) with a well-developed Bw horizon (b10Bw). Between the depths of 90 and 95 m the last rubified pedocomplex, which has developed on loess is found forming two Bw horizons (U2-S11, U2-S12). From 97 down to 100 m, the base of the LPS is given by a pedocomplex of very high clay content and dark red hue (U2-S13). This pedocomplex is formed on the underlying red clays of the Tengelic Clay Formation.

#### 4.2. Magnetic susceptibility values

Mass specific magnetic susceptibility ranged between 6 and 225

$\cdot 10^{-8} \text{m}^3 \text{kg}^{-1}$  in the entire profile with a mean of  $49.42 \cdot 10^{-8} \text{m}^3 \text{kg}^{-1}$ , median of  $24 \cdot 10^{-8} \text{m}^3 \text{kg}^{-1}$  and a positive skewness (SD: 37.51, SK: 2.35, K: 6.25) implying that most values are low in accordance with the relatively thick loess deposits and thin intercalated paleosols in terms of total thickness. (Supplementary Fig. 3). A polymodal distribution with a right tail approximating a Gamma type distribution again corroborates the action of multiple processes in the formation of the studied LPS (Supplementary Fig. 4).

In most Danubian and Chinese loess profiles, magnetic susceptibility ( $\chi$ ) seems to show a positive correlation with the intensity of pedogenesis as a result of precipitation of more very fine-grained so-called superparamagnetic minerals forming during the process of pedogenesis yielding higher values for paleosols compared to loess (Bugge et al., 2009, 2013; Marković et al., 2011, 2015; Fitzsimmons et al., 2012). This type of relationship follows the so-called pedogenetic enhancement model of susceptibility (Kukla et al., 1980; Heller and Liu, 1982, 1984; Zhou et al., 1990; Maher, 1998; Ding et al., 2005).

Occurrence of atypical MS patterns is attributable to various factors. On the one hand, increased humidity resulting in water-logging and moist oxidizing or even reducing conditions leads to transformation of the ferromagnetic content, a reduction of  $\chi$  and thus a negative correlation between  $\chi$  and pedogenesis (Chlachula et al., 1997, 1998; Liu et al., 1999, 2007, 2012; Matasova et al., 2001; Heil et al., 2010). Likewise, when climatic conditions prevail around a threshold between loess formation and initial pedogenesis due to say enhanced physical weathering or high seasonal variability affecting hematisation, a similar negative correlation between  $\chi$  and pedogenesis is observed (Guo et al., 2011; Song et al., 2010; Liu et al., 2012). Variations between these possibilities can appear in a single profile depending on conditions of ferromagnetic mineral production.

The weakly developed paleosols with low susceptibility signal ( $19\text{--}25.5 \cdot 10^{-8} \text{m}^3 \text{kg}^{-1}$ ) (U2S2, U2S5) as well as loess layers ( $6\text{--}19 \cdot 10^{-8} \text{m}^3 \text{kg}^{-1}$ ) were assigned to Group 1 based on cluster analysis. U2-S2 is lacking pedological features indicating humidity

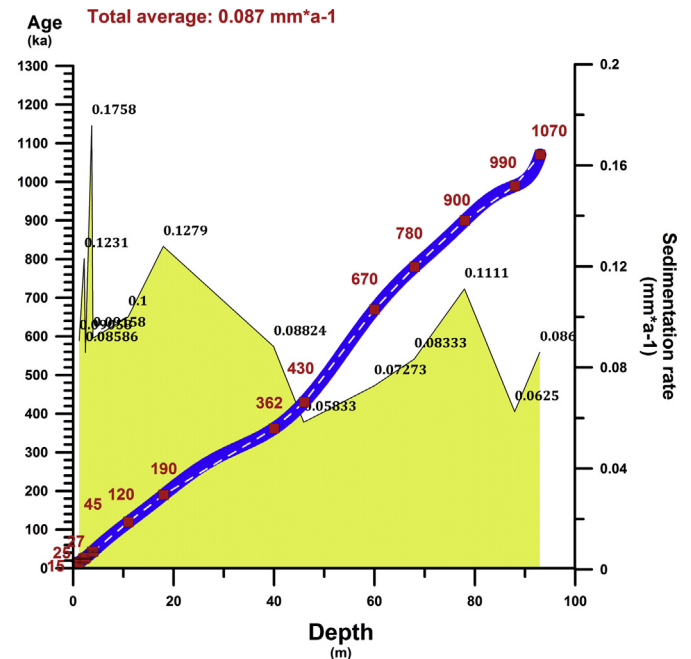


Fig. 5. Age-depth model for the studied core and calculated sedimentation rates between major age-tiepoints.

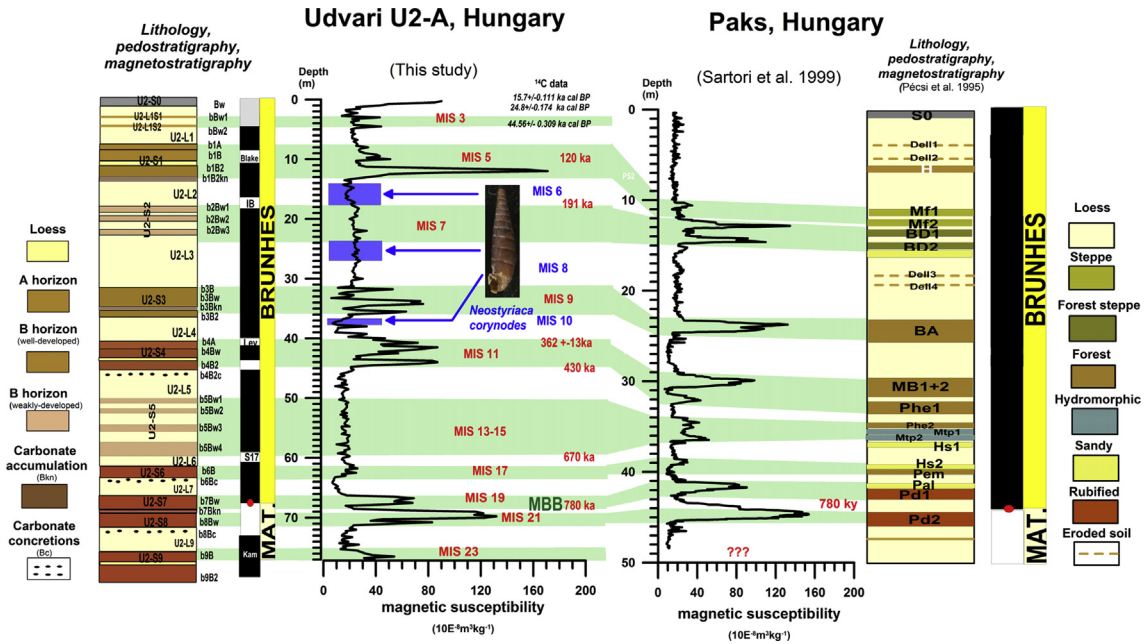


Fig. 6. Interprofile correlation of the Hungarian site of Paks (Pécsi et al., 1995; Sartori, 2000; Sartori et al., 1999) and borehole Udvari-2A based on litho-, pedo-, magneto-, biostratigraphy as well as mass-specific magnetic susceptibility.

controlled signal destruction (Fig. 3). Thus a threshold between loess deposition and paleosol formation must be blamed for the low value. Conversely, hydromorphic features noted in the lower part of the weakly developed U2-S5 pedocomplex, also characterized by a weak  $\chi$  signal of similar range, hints to a humidity-induced transformation of ferromagnetic minerals. The well-developed U2-S6 paleosol with very low  $\chi$  values ( $\sim 25 \cdot 10^{-8} \text{m}^3 \text{kg}^{-1}$ ) was also put in Group 1 implying that special conditions must have resulted here in signal loss. (Fig. 3). At the stratigraphic position of our U2-S6 pedocomplex, there are embryonic (Paks Embryonic Soil: PEM) and sandy soils (Paks Sandy Soil: Hs2)

in the nearby Paks profile, which are characterized by likewise low MS values of similar ranges (Fig. 7) (Sartori et al., 1999; Sartori, 2000). Low susceptibility values of the paleosols at Paks are thus most likely the outcome of increased physical weathering and deposition as seen from the lithology. However, the corresponding V-S6 paleosol in Vojvodina is likewise well-developed despite having similarly weak susceptibility values (Fig. 8) as the U2-S6 soil (Marković et al., 2008, 2011). Correspondence between the V-S6 paleosol at Stari Slankamen and U2-S6 paleosol at Udvari 2A is not only stratigraphical but also corroborated by independent paleomagnetic data as presented in section 4.3. Weak values here are

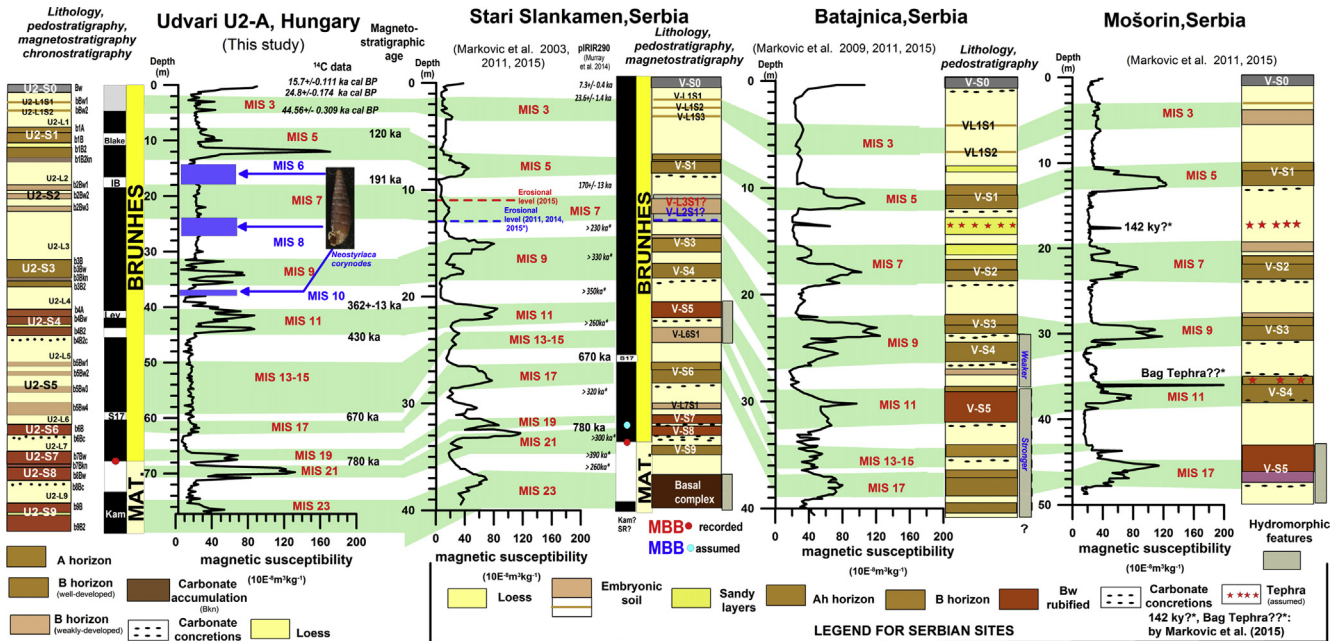


Fig. 7. Interprofile correlation of the borehole Udvari-2A with Serbian profiles of Stari Slankamen (Marković et al., 2011, 2015; Murray et al., 2014), Batajnica (Marković et al., 2009, 2011, 2015) and Mošorin (Marković et al., 2012a, 2015) based on litho-, pedo-, magneto-, biostratigraphy as well as mass-specific magnetic susceptibility.

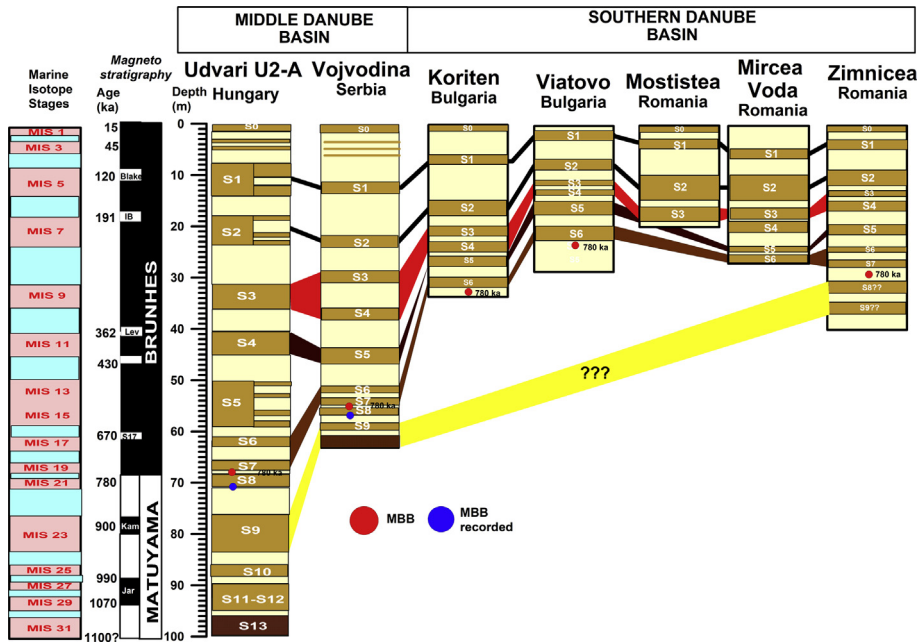


Fig. 8. Interprofile correlation of selected Middle Danube Basin and Lower Danube Basin loess paleosol sequences.

thus most likely due to seasonal variability affecting the hematization process rather than climate change (Fitzsimmons et al., 2012). Group 2 with values between 25 and 85  $\cdot 10^{-8} \text{m}^3 \text{kg}^{-1}$  included more developed interglacial paleosol of U2-S3, U2-S4, U2S7, with thick B and Bw horizons, the modern soil U2-S0 (Fig. 3), also belongs here. Samples with  $\chi$  values above 85  $\cdot 10^{-8} \text{m}^3 \text{kg}^{-1}$  form 2 groups. Group 3 (86–126  $\cdot 10^{-8} \text{m}^3 \text{kg}^{-1}$ ) as outliers represents the rubified paleosols U2-S8, U2-S11 and U2-S12, while Group 4 (126–225  $\cdot 10^{-8} \text{m}^3 \text{kg}^{-1}$ ) (Supplementary Fig. 3) corresponds to the last interglacial paleosol U2-S1 and the chromic pedocomplexes U2-S9 and U2-S10. (Fig. 3, Supplementary Fig. 3).

#### 4.3. Magnetostratigraphy

Márton (1998) identified two normal (C1n and C2n) and two reversed polarity (C1r and C2r) chronozones for the entire borehole sequence (Fig. 2). The bottom part between the depths of 71 and 125 m is characterized by reversed polarity (C1r) representing the upper part of the Matuyama Chron with several short normal polarity excursions recorded. Within the Matuyama Chron, the excursion corresponding to the Olduvai Subchron (1.77–1.95 Ma) (C2n) was located in the borehole between the depths of 124 and 137 m (Fig. 2 and Table 2.). While another major normal excursion between the depths of 88.3 and 93.3 m was interpreted to represent the Jaramillo Subchron lasting for ca. 80 ka dated between 0.99 and

1.07 Ma. (Márton, 1998; Koloszár, 2003; Koloszár and Marsi, 2010a; b). A short lived normal polarity zone between the depths of 77 and 80 m below the MBB may represent the Kamikatsura (0.86–0.9 Ma) excursion based on its stratigraphic position (Figs. 2 and 3 and Table 2). The boundary of C1n and C1r was considered to represent the MBB. From the chronological point of view, the position of the Matuyama-Brunhes Boundary (MBB) is a good reference point in our profile. It was located between two rubified paleosols (U2-S7, U2-S8, Fig. 3) but at a depth of 71 m, which is under the lower of the two paleosols in our revised stratigraphy (Márton, 1998; Koloszár, 1997, 2003; Koloszár and Lantos, 2001; Koloszár and Marsi, 2010a; b). If we accept that the MBB is between the two paleosols (U2-S7 and U2S8) then the displacement could indicate the so-called lock-in depth effect noted in other Chinese and Danubian loess profiles as well (Zhou and Shackleton, 1999; Marković et al., 2011, 2015; Murray et al., 2014). A similar depth and position for the MBB was noted for the Xifeng loess section above loess unit 8 (L8) at a depth of 71 m. Later a higher position of MBB above the S8 pedocomplex and the bottom of S7 was proposed at a depth of 69 m for this profile (Liu et al., 1987, 1988; 2008; Guo et al., 2011, 2009a; b; Sun et al., 2009; Wu and Wu, 2011). The displacement of the MBB from the top of L8 towards the bottom of S7 have been noted by Zhou and Shackleton (1999) blaming the so-called lock-in effect for the original position of the boundary. More recently detailed studies of  $^{10}\text{Be}$  at both Xifeng and Luochuan found that the MBB is actually recorded in the paleosol S7 (~67 m in Xifeng) corresponding to MIS 19, corroborating that the Chinese loess magnetic susceptibility time-scale is correct for the mentioned profiles (Zhou et al., 2014).

Likewise, in the nearby site of Paks the MBB was initially located below (Pécsi and Pevzner, 1974; Márton, 1979) the rubified Paks Double Pedocomplex (PD1, PD2). Later it was placed between the two members of this pedocomplex at a depth of 44 m (Sartori et al., 1999; Sartori, 2000). If PD1 (Table 1) can be correlated with the S7 soil in the Chinese profiles, then the position of the MBB both at Paks and in Udvari-2A is in line with those records. Similar stratigraphic position of the MBB was noted in several other Transdanubian profiles and boreholes too, although at varying depths

Table 2  
The position of recorded geomagnetic excursions in the borehole Udvari-2A.

International Geomagnetic Polarity Scale	Depth (m)	Event
BRUNHES	9–11	Blake
	18–20	Iceland Basin
	40–41	Levantine
	45–46	Unnamed
	59–61	Stage 17
	68–73	MBB
MAT	77–80	Kamikatsura
	88.3–93.3	Jaramillo
	124–137	Olduvai

**Table 3**  
Results of radiocarbon analysis of the upper 4 m of the profile.

Sample depth (m)	Sample code	Dated material (Mollusk taxa)	Lab code	14C age (yr BP)	$\pm 1 \sigma$	2 $\sigma$ calibrated age ranges (cal BP, 95.4% prob.)			
						Min	Max	Mean	$\pm 1 \sigma$
1.25	UD-1	<i>Chondrula tridens</i> (Müller, 1774)	D-AMS 01443	13,290	42	15790	16160	15979	93
1.25	UD-2	<i>Granaria frumentum</i> (Draparnaud, 1801)	D-AMS 01444	13,091	45	15460	15930	15702	111
2	UD-3	<i>Arianta arbustorum</i> (Linnaeus, 1758)	D-AMS 01445	20,598	77	24481	25138	24803	174
2	UD-4	<i>Chondrula tridens</i> (Müller, 1774)	D-AMS 01447	20,193	66	24038	24481	24259	112
2.25	UD-5	<i>Granaria frumentum</i> (Draparnaud, 1801)	D-AMS 01446	21,212	81	25306	25771	25555	116
2.5	UD-6	<i>Granaria frumentum</i> (Draparnaud, 1801)	D-AMS 01448	23,380	90	27406	27762	27586	90
3.75	UD-7	<i>Granaria frumentum</i> (Draparnaud, 1801)	D-AMS 01449	37,849	277	41735	42556	42144	205
4	UD-8	<i>Bradybaena fruticum</i> (Müller, 1774)	D-AMS 01450	39,905	300	42993	44198	43566	309

Conventional 14C ages have been calibrated using OxCal 4.2 and the IntCal13 calibration curve.

(Kolozsár and Lantos, 2001).

Several short and almost complete changes in geomagnetic inclination have occurred within the Brunhes chron represented by the upper 71 m of our profile (Fig. 3, Table 2.). A reversed polarity zone sitting above the MBB in our borehole at the depth of 59–61 m (Fig. 3, Table 2.) based on its stratigraphic position corresponds to the so-called “Stage 17” excursion event (670–685 ka) (Biswas et al., 1999; Channel and Raymo, 2003; Laj and Channel, 2009; Channell et al., 2010; Singer, 2014; Singer et al., 2014). A magnetic reversal noted at roughly the same stratigraphic position above the S6 soil in the Vojvodinian site of Stari Slankamen was likewise interpreted as the stage 17 excursion (Hambach et al., 2009; Marković et al., 2011; Marković et al., 2015.). A reversal reported from borehole Ūh-2 of SW Transdanubia at a depth of ca. 46 m (Marsi et al., 2004) may also represent this excursion.

The two reversed polarity events at depths of 46 and 40 m represent (Fig. 3, Table 2.) the unnamed event at 430 ka and the Levantine excursion dated around 362 $\pm$ 13 ka marking the boundaries of MIS 11 (Langereis et al., 1997; Lund et al., 2001, 2006; Laj and Channel, 2009; Michalk et al., 2013). These reversed geomagnetic excursions bracketing MIS 11 are also present in the paleomagnetic record of the latest INQUA 2016 Global chronostratigraphical correlation table for the past 2.7 ma<sup>1</sup> (Cohen and Gibbard, 2016), although not named. Further verification of our interpretation comes from biostratigraphy presented below. The short-lived reversed polarity event at a depth of 18 m represents the MIS6/MIS7 transition (Iceland Basin excursion at 191 ka) based on its biostratigraphically controlled stratigraphic position (see below). The excursion at the depths between 9 and 11 m in our profile (Fig. 3 and Table 2.) was originally thought to represent the Laschamp event (41 ka). Thus, Kolozsár and Marsi (2010a, b) assigned the uppermost paleosol (Ps1 according to their stratigraphy, U2-S1S1 according to the new stratigraphy) to MIS 3 by correlating the MS susceptibility curve with the marine curve of Crowhurst (2002) (Fig. 2). According to the newly gained radiocarbon dates, this idea can be rejected as the last 42 ka is restricted to the upper 4 m of the profile. It is important to note that this part of the sequence was not subjected to paleomagnetic investigations (Márton, 1998). So, based on our records we infer this event represents the Blake excursion dated at 120 ka (Singer, 2014; Singer et al., 2014).

#### 4.4. <sup>14</sup>C ages

Table 3 presents the received conventional <sup>14</sup>C ages with 1  $\sigma$  error for samples between 1.25 and 4 m in addition to the 2  $\sigma$

calibrated age ranges (95.4% probability). Samples UD-1, UD-2 were taken from similar depths corresponding to different gastropod taxa listed in Table 3. This also applies to samples UD-3 and UD-4. According to our results, the uppermost 4 m represents the last 43–44 ky. MIS 2 (28–14.65 ka cal BP) is broadly represented by the interval 1.25–2.5 m, and the underlying interval to 4 m depth represents the majority of MIS 3 (58–28 ka cal BP).

#### 4.5. Biostratigraphy

The first appearance of the Middle Pleistocene index fossil *Neostyriaca corynodes* in our profile was recorded in the loess at a depth of 37.5 m (U2-L4) (Fig. 6). This loess unit thus corresponds to the *Helicigona vertesi* biozone (Krolopp, 1973, 1977; 1994) and MIS 10, sitting right on top of a pedocomplex (U2-S4) bracketed by the Levantine (362 $\pm$ 13 ka) excursion and the unnamed event of 430 ka (Langereis et al., 1997; Lund et al., 2001, 2006; Laj and Channel, 2009; Michalk et al., 2013) (see prev. section). The next two occurrences of this taxon are found in loess units between the depth of 24–27.5 m (U2-L3) and 15–18 m (U2-L2), respectively (Fig. 6). The bottom of the uppermost occurrence is within the Iceland Basin (191 ka) excursion marking the MIS 6/MIS 7 boundary. As the second most prominent appearance of this taxon is dated between 180 and 140 ka (MIS 6) in general (Sümegei et al., 2002, 2011a; Sümegei and Krolopp, 2006; Sümegei, 2007) this upper loess unit (U2-L2) can clearly be assigned to MIS 6. This is further corroborated by independent magnetostratigraphic data. An absence of this taxon between the two loess units at 18–23.5 m corresponds stratigraphically with a paleosol (U2-S2), which was overlooked by Kolozsár (1997) and Kolozsár and Marsi (2010a,b). *Neostyriaca corynodes* is found together with interglacial elements upwards from the upper boundary of the upper loess unit (U2-L2) between the interval of 14–13 m. This is a clear mark of a transition to an interglacial. A similar mixed fauna is present in the upper parts of loess unit U2-L3 (18–20 m) marking another glacial-interglacial transition. Thus, we infer the two uppermost occurrences of *N. corynodes* bracket interglacial paleosols. The age of the upper interglacial paleosol (U2-S1) is independently determined by the location of the Blake excursion (120 ka) (MIS 5). As it was noted in section 3.3, there is a third intermediate temporal occurrence of this taxon recorded in some boreholes and outcrops (Klemm, 1969; Krolopp, 2005) corresponding to MIS 8. So, its presence between 24 and 27.5 m clearly assigns the loess U2-L4 into MIS 8. Occurrences of another Lower and Middle Pleistocene interglacial taxon *Mastus bielzi* (Krolopp, 2003; Sümegei et al., 2011b) in the paleosol horizons of U2-S4, U2-S6, U2-S7 and U2-S8 further corroborates the Lower and Middle Pleistocene age of these referred paleosols.

<sup>1</sup> <http://www.stratigraphy.org/upload/QuaternaryChart.pdf>.

#### 4.6. Age-depth models and MARs

The prepared age-depth model for the upper 4 m is presented on Fig. 4. The calculated average sedimentation rates for the MIS 2 part of the section were  $0.11 \text{ mm} \cdot \text{a}^{-1}$ , yielding a MAR of  $169 \text{ g} \cdot \text{m}^{-2} \cdot \text{a}^{-1}$  (Fig. 4). This rate is lower than the calculated average for MIS 2 of the Carpathian Basin (SR:  $0.28 \text{ mm} \cdot \text{a}^{-1}$ , MAR:  $417 \text{ g} \cdot \text{m}^{-2} \cdot \text{a}^{-1}$ ) (Újvári et al., 2010). All these imply that the coldest period of the last glacial cycle (MIS 2) here was characterized by relatively low accumulation rates compared to other late glacial deposits from Southern Hungary. Yet accumulation rates are similar to recorded values at the other deep profile of Vojvodina dating back 1 My: Stari Slankamen (SR:  $0.11 \text{ mm} \cdot \text{a}^{-1}$ , MAR:  $168 \text{ g} \cdot \text{m}^{-2} \cdot \text{a}^{-1}$ ) (Újvári et al., 2010; Marković et al., 2011, 2015). It may indicate similar tectonic, accumulation histories and/or a similar plateau position of these two “antique” sites during the coldest period of the last glacial cycle. Somewhat higher, but still very similar accumulation rates were documented for the nearby site of Ságvár (SR:  $0.12 \text{ mm} \cdot \text{a}^{-1}$ , MAR:  $176 \text{ g} \cdot \text{m}^{-2} \cdot \text{a}^{-1}$ ) for the period between 21,030–22,700 cal BP, and the more distant sites of Erdut, Croatia (SR:  $0.14 \text{ mm} \cdot \text{a}^{-1}$ , MAR:  $215 \text{ g} \cdot \text{m}^{-2} \cdot \text{a}^{-1}$ ), Crvenka, Serbia (SR:  $0.13 \text{ mm} \cdot \text{a}^{-1}$ , MAR:  $197 \text{ g} \cdot \text{m}^{-2} \cdot \text{a}^{-1}$ ), and Irig, Serbia (SR:  $0.13 \text{ mm} \cdot \text{a}^{-1}$ , MAR:  $192 \text{ g} \cdot \text{m}^{-2} \cdot \text{a}^{-1}$ ) (Újvári et al., 2010). Based on this information we infer an essentially spatially uniform dust accumulation across the region represented by these sites during MIS 2. However, when we look at the sedimentation rates within MIS 2 and MIS 3 the picture is somewhat different (Fig. 5) From about 29 ka there is a marked twofold increase in dust accumulation culminating during the middle part of the LGM at a value of  $0.1936 \text{ mm} \cdot \text{a}^{-1}$  (MAR:  $290 \text{ g} \cdot \text{m}^{-2} \cdot \text{a}^{-1}$ ). Yet this almost two-times higher than the average MIS 2 value of our profile is still below that of the MIS 2 average of the Carpathian Basin (SR:  $0.28 \text{ mm} \cdot \text{a}^{-1}$ , MAR:  $417 \text{ g} \cdot \text{m}^{-2} \cdot \text{a}^{-1}$ ) (Újvári et al., 2010).

The age-depth model constructed using the most reliable magnetostratigraphic tiepoints (120 ka, 191 ka,  $362 \pm 13$  ka, 430 ka, 780 ka, 900, 990 ka, 1.07 Ma) complemented by calibrated  $^{14}\text{C}$  dates is presented on Fig. 5. The overall calculated sedimentation rate was  $0.087 \text{ mm} \cdot \text{a}^{-1}$  for the entire profile, which is similar to the estimated sedimentation rates of  $0.078\text{--}0.08 \text{ mm} \cdot \text{a}^{-1}$  of the Xifeng and Chanwu loess paleosol sequences (Liu et al., 1987, 1988). Based on the literature, the thick loess deposits of Central China have accumulated at an average rate of 0.1 m/ka which is comparable to our calculated accumulation rate for the entire profile (Banerjee and Jackson, 1996; Rapp, 2012).

Within the Matuyama chron sedimentation rates were decreasing during the Jaramillo subchron between 1070 and 990 ka to  $0.0625 \text{ mm} \cdot \text{a}^{-1}$  in line with the formation of two chromic paleosols (U2-S12, U2-S11). There is an almost twofold increase in accumulation rates between 990 and 900 ka reaching a value of  $0.11 \text{ mm} \cdot \text{a}^{-1}$ . It's interesting to see that this value is in the range of those of glaciials after MIS 11. From here there is a gradual decrease up to about mid-depth of the profile (43 m), corresponding to the time of the Mid-Brunhes transition (MBE) (Jansen et al., 1986; Yin et al., 2008; Yin, 2013), to values around  $0.05833 \text{ mm} \cdot \text{a}^{-1}$ . This value is almost the same as that within the Jaramillo subchron. The key characteristic of the MBE is a shift from low-magnitude, relatively subdued or muted glacial/interglacial cycles during the Early Middle Pleistocene (EMP) to extreme and large-scale Late Middle Pleistocene (LMP) glacial/interglacial cycles from MIS 11 onwards. In accordance with global records showing a stepwise change to warmer climates with longer interglacials (Lisiecki and Raymo, 2005; Jouzel et al., 2007) and higher atmospheric concentrations of carbon dioxide and atmospheric dust (Hovan et al., 1991; Lüthi et al., 2008; Lambert et al., 2012), there is a stepwise change in the accumulation rates following the Mid-Brunhes transition to

values ranging between  $0.10$  and  $0.12 \text{ mm} \cdot \text{a}^{-1}$  on average up to about MIS 6. Highest accumulation rates characterize the glaciials of MIS 10, MIS 8, MIS 6.

### 5. Comparison with other middle dabune basin profiles of the same age

#### 5.1. Correlation with the nearby Paks profile

Fig. 6 presents an interprofile stratigraphic correlation of the two Hungarian sites of borehole Udvari- 2A and Paks brickyard based on the newly established chronostratigraphy for the former section. From Udvari, only the part down to MBB has been used as the record in Paks does not extend further than that. In case of Paks three sampled sites are presented (Supplementary Fig. 5). The rightmost (Pécsi et al., 1995; Sartori et al., 1999; Sartori, 2000) represents the so-called INQUA profile facing east on the banks of the River Danube. The center (Thiel et al., 2014) was located at the southern margin of the now closed brickyard facing NE. The exact orientation and position of the third leftmost site is not described in detail (Újvári et al., 2014a).

The 49-m loess/paleosol sequence of the INQUA profile at Paks is divided into a “Young Loess Series (YLS)” (upper 29.3 m, MIS 2–10) and an “Old Loess Series (OLS)” (lower 19.7 m, MIS 11–22) (Pécsi, 1975, 1993; 1995; Pécsi et al., 1995; Sartori, 2000; Gábris, 2007; Újvári et al., 2014a). This division is presented in the two additional profiles too (Thiel et al., 2014; Újvári et al., 2014a). The profile of Újvári et al. (2014a) spans an interval of 45 m. Conversely, Thiel et al. (2014) focused on the interval capturing the upper part of the profile down to the so-called BA paleosol and the underlying loess to a depth of ca. 22 m.

In our correlation, the primary focus was on the original INQUA profile presented in Pécsi (1995), Pécsi et al. (1995), Sartori (2000) and Sartori et al. (1999). Additional remarks are also made within the text regarding the remaining referred two profiles of Újvári et al. (2014a) and Thiel et al. (2014). In contrast to traditional correlations starting from the top, our work starts at the bottom. The reason is the location of the only reliable chronological reference point in the Paks profile: the MBB at the depth of 44 m (Fig. 6).

The bottom part of the profile of Paks between the depths of 45.2–48.9 m consists of moderately structured loess containing carbonate concretions of the overlying Pd2 paleosol in its upper parts. The  $\chi$  values range between  $10$  and  $20 \cdot 10^{-8} \text{ m}^3 \text{ kg}^{-1}$  (Sartori et al., 1999; Sartori, 2000). In the studied Udvari- 2A borehole sequence, the corresponding unstratified, medium-compacted pale yellow loess of U2-L9 in the depths of 73–76 m (Kolozsár, 1997; Kolozsár and Marsi, 2010a; b) likewise contains calcareous nodules of 1–8 cm size in its upper parts (b8Bc) deriving from the overlying pedocomplex (U2-S8). The  $\chi$  values are comparable with a range between  $12$  and  $29 \cdot 10^{-8} \text{ m}^3 \text{ kg}^{-1}$  for this part.

The first paleosol at U2-A directly below the MBB is a 2-m thick rubified compacted paleosol (U2-S8) with a well-developed B horizon (b8BW) and the second highest  $\chi$  value of  $132 \cdot 10^{-8} \text{ m}^3 \text{ kg}^{-1}$  in the sequence. This paleosol corresponds stratigraphically to the reddish chestnut steppe soil Pd2 at Paks, which is likewise located below the MBB and has a similar thickness of ca. 2 m (Pécsi et al., 1995; Sartori et al., 1999; Sartori, 2000). Its highest  $\chi$  value is around  $150 \cdot 10^{-8} \text{ m}^3 \text{ kg}^{-1}$  (Sartori, 2000; Sartori et al., 1999). The overlying chestnut soil of Pd1 at Paks between the depth of 41.2–42.3 m with a thickness of 1 m has lower  $\chi$  values between  $80 \cdot 10^{-8} \text{ m}^3 \text{ kg}^{-1}$  and  $90 \cdot 10^{-8} \text{ m}^3 \text{ kg}^{-1}$  (Sartori et al., 1999; Sartori, 2000) compared to Pd2. It seems to show a strong similarity to the rubified paleosol U2-S7 of our borehole sequence both in terms of pedological characteristics, thickness (1.1 m) and lower  $\chi$  values ( $72 \cdot 10^{-8} \text{ m}^3 \text{ kg}^{-1}$ ) compared to the underlying paleosol (U2-S8). The

Pd2 and Pd1 paleosols were also recorded in the profile of Újvári et al. (2014a) at shallower depths.

The next unit termed as Paks alluvial soil is missing both in Udvari 2-A and the profile of Újvári et al. (2014a). The following paleosol unit above U2-L7 in our borehole sequence (U2-S6) at the depths of 61–63 m has a total thickness of 1 m and a strongly reduced  $\chi$  value  $25\text{--}26 \cdot 10^{-8} \text{m}^3 \text{kg}^{-1}$ . Similar  $\chi$  values were observed for the embryonic soils of Paks (Pem + Hs2) found in the same stratigraphic position at depths between 38.4 and 39.4 m (Fig. 6). Not to mention the same thickness of the corresponding paleosols. These referred units are completely missing in the profile of Újvári et al. (2014a). As the U2-S6 paleosol has a relatively well developed reddish brown B horizon with underlying carbonate accumulation zone, low MS values must be due to the destruction of ferromagnetic minerals by high seasonal variation as mentioned in section 4.2. In case of the corresponding Paks paleosols, the observed lithological features hint to a destruction of the signal via continuous bleaching from dust and sand accumulation. Based on the independent chronostatigraphy for Udvari-2A using the stage 17 excursions these paleosols were formed during MIS 17.

The overlying pedocomplex in Paks is represented by weakly developed sandy soils (Hs1 and Phe 2) and moderately developed luvisols (hydromorphic gallery forest type soils) (Mtp 1–2) of low MS values ranging from  $18$  to  $40 \cdot 10^{-8} \text{m}^3 \text{kg}^{-1}$  (Pécsi, 1995; Pécsi et al., 1995; Sartori et al., 1999; Sartori, 2000). Similarly, low values were noted by us in the Udvari-2A borehole profile just above the U2-S6 soil. Koloszar and Marsi (2010a,b) interpreted this unit as infusion or marshy loess. However, this can be refuted based on the complete lack of freshwater mollusks (Sümegei et al., 2015). The U2-S5 pedocomplex between the depths of 50 and 59 m corresponding to the Hs1 and Phe2 is made up of several weakly developed soils (b5Bw1–b5Bw4). The upper ones have moderate clay and some sand content (b5Bw1, b5Bw2), while the lower (b5Bw3, b5Bw4) have higher clay content and display some hydromorphic characteristics. No signs indicating the presence of pseudogley was noted. Rather pedogenetic processes creating reducing conditions are to blame for the destruction of the original magnetic signal. Units Hs1 and Phe 2 were not recorded by Újvári et al. (2014a). In the horizon corresponding to the upper part of the U2-S5 pedocomplex three paleosols are noted in Paks (Mtp1, Mtp2, Phe2). Mtp1 was originally interpreted as a steppe soil with ca. 30% sand and clay content. Mtp2 on the other hand, was initially considered as a dark brown, strongly clayey meadow chernozem (Pécsi, 1995). Sporadic occurrences of mottling and a high clay content was also observed. Pécsi later changed this to a gleyed hydromorphous soil (Pécsi et al., 1995), which was adopted by later studies as lessive-pseudogley (Bronger, 2003) or pseudogley (Újvári et al., 2014a; Varga, 2012). Újvári et al. (2014a) identified this unit roughly at the same depth as Pécsi (1995). To avoid further confusions in correlation, it must be emphasized that Pécsi made his statement on the basis of the recorded low MS values atypical of the ones observed for chernozem soils (Pécsi et al., 1995; Sartori, 2000). In addition, neither Bronger (2003), nor Újvári et al. (2014a) presented detailed pedological, sedimentological evidence for their interpretation. In previous works (e.g. Bronger, 2003; Gábris, 2007; Varga, 2011, 2012; Újvári et al., 2014a) the Mtp1 and Mtp2 paleosols at Paks were correlated with MIS 13–15. But this correlation so far was rather tentative based on the interpreted stratigraphic position of the MBB (Újvári et al., 2014a,b). As the pedocomplex U2-S5 is clearly bracketed by two geomagnetic excursions above U2-S6 and below U2-S4 at Udvari-2A, the correlation of the referred corresponding Paks paleosol units with MIS 13–15 is now independently justified.

The pedocomplex composed of the chestnut polygenetic brown earth soil (MB2), the overlying weakly developed forest steppe soil

(MB1) and the underlying light grey weakly developed sandy forest soil (Phe1) with a total thickness of 4 m between the depth of 29 and 33 m seem to correspond to the U2-S4 pedocomplex of similar thickness. Although the lower sandy member of the Paks S4 pedocomplex (Ph1) has low susceptibility values around  $50 \cdot 10^{-8} \text{m}^3 \text{kg}^{-1}$ ,  $\chi$  values for the upper members (MB 1 + 2) are only somewhat higher ( $110 \cdot 10^{-8} \text{m}^3 \text{kg}^{-1}$ ) than the U2-S4 pedocomplex at Udvari ( $90 \cdot 10^{-8} \text{m}^3 \text{kg}^{-1}$ ). These high values clearly indicate a pedogenetic origin paleomagnetic signal acquisition and well-developed paleosols in accordance with lithostratigraphical and pedostratigraphical descriptions for Udvari in section 4.1. The similar shape of the susceptibility curves further support the idea of integrating the MB 1 + 2 and Ph1 paleosols into a single pedocomplex. Based on initial TL data for Paks, the MB pedocomplex was formerly correlated with MIS 5 (Borsy et al., 1979; Butrym and Maruszczak, 1984), which was later refuted by other TL studies yielding ages older than 315 ka (Wintle and Packman, 1988; Singhi et al., 1987; Zöller and Wagner, 1990). Kukla (1977) put the base of the MB soil around 500 ka based on magnetostratigraphy. As a supporting evidence the presence of *Elephas trogontherii*, a middle-Pleistocene mammal, in the loess below the MB soil horizon was also cited (Kukla, 1977). The correlation of MB paleosol at Paks with MIS 11 was presumed by Bronger (2003). However, his correlation with the FIV paleosol of Karamaydan and the S4 paleosol of Luochuan was based partly on the unified pedostratigraphic scheme of the 1962 INQUA and two control points, the position of the geomagnetic horizon corresponding to the MBB, and the location of the F3 paleosol representing MIS 5. A further presumption was that climatic changes at the scale of glacial interglacials are synchronous on the northern hemisphere (Bronger, 2003). Oches and McCoy (1995 a,b) also correlated the MB pedocomplex with MIS 11 based on AAR results. Our findings for Udvari-2A clearly assign this pedocomplex (MB1+2 and Ph1) to MIS 11 based on the geomagnetic polarity reversals bracketing the corresponding U2-S4 paleosol and biostratigraphic data for the overlying MIS 10 loess (U2-L4) (Fig. 6).

The chestnut, chocolate colored, well-developed, structured forest steppe paleosol BA at Paks at depths of 23.3–25.1 m have higher  $\chi$  values of  $130\text{--}140 \cdot 10^{-8} \text{m}^3 \text{kg}^{-1}$  than the underlying S4 pedocomplex (Mtp1+2, Phe1). An opposite trend is observed for the Udvari-2A borehole, where the corresponding S3 pedocomplex (U2-S3) representing MIS 9 has somewhat lower  $\chi$  values of  $70\text{--}80 \cdot 10^{-8} \text{m}^3 \text{kg}^{-1}$  than the underlying S4 soil (U2-S4). This may tentatively indicate a change in conditions between the two sites after about 400 ka, representing the Mid-Brunhes event. Kukla (1977) put the age of the BA paleosol around 400 ka. TL and IRSL studies at Paks gave ages >190ka (Singhi et al., 1987; Zöller and Wagner, 1990; Frechen et al., 1997). Oches and McCoy (1995 a,b) presumed a correlation with MIS 9 based on AAR data. Thiel et al. (2014) considered the BA paleosol to most likely represent MIS 9 based on pIRIR290 measurements. Observation of the stratigraphic position of the Bag Tephra in the loess below this paleosol by Thiel et al. (2014) further corroborates their assumption (Supplementary Fig. 5).

As in the Udvari-2A sequence the U2-S3 paleosol corresponding to BA in Paks is bracketed by the MIS 10 and MIS 8 occurrences of *Neostyriaca corynodes*, the MIS 9 age of the referred paleosols can be further corroborated. Independent occurrences of this biostratigraphic marker element at the nominating site of the BA paleosol Basaharc north of Budapest along the Danube in the same stratigraphic position below the BA paleosol (Sümegei, 1991; Sümegei and Krolopp, 2005, 2006; Sümegei et al., 2011a) renders further support. In addition, *Neostyriaca corynodes* also turns up in SE Transdanubia below the BA paleosol at several nearby sites of Dunaszentgyörgy, Dunaszekcső, Mórág (Hum and Sümegei, 2000,

2001; Hum, 2002, 2005, 2007). In some cases, even the collective occurrences of the Bag Tephra and *Neostyriaca corynodes* was also recorded (Hum and Sümeği, 2000, 2001; Hum, 2002, 2005, 2007) further corroborating the MIS 9 age of the BA paleosol.

The next greyish brown weakly and moderately developed steppe soils of BD1 and BD2 at Paks corresponds to the Udvari the U2-S2 pedocomplex (Fig. 6). U2-S2 is weakly developed and does not turn up univocally on the MS curve (see section 4.2). According to Horváth and Bradák (2014) the corresponding Basaharc Double paleosols (BD1+BD2) are also weakly or moderately developed compared to the overlying younger or underlying older interglacial paleosols. In addition, these forest, forest steppe and chernozem type soils were mentioned to have a local hydromorphic character (Horváth and Bradák, 2014). This would explain observations of a weakly developed pedocomplex with diminished magnetic susceptibility values for the MIS 7 paleosol (U2-S2) in our profile.

The BD1+BD2 pedocomplex in Thiel et al. (2014) profile was corroborated to represent MIS 7 based on pIRIR290 luminescence based geochronological investigations done by the same study. Despite Pécsi's early interpretation of this pedocomplex being representative of the last glacial cycle interstadials, the age of the pedocomplex at the Basaharc type section was determined to be Middle Pleistocene age (MIS 7) on the basis of TL investigations (Wintle and Packman, 1988; Zöller and Wagner, 1990) and the appearance of the biostratigraphic marker gastropod *Neostyriaca corynodes* in the underlying loess (Sümeği, 1991; Sümeği and Krolopp, 2005, 2006; Sümeği et al., 2011a). The loess unit overlying the BD pedocomplex at Paks is made up of fine sandy loess, typical loess and sand layers (16 and 23 m), interpreted as a typical layered sandy slope loess with two erosional horizons (Dell 3, 4) between 18 and 20 m. Reworked soil was also observed between 22.3 and 23.3. Two erosional horizons were recorded by Thiel et al. (2014) as well most likely corresponding to Dell 3–4.

The uppermost chestnut steppe soils representing the last interglacial MF1 and MF2 (Wintle and Packman, 1988; Singhvi et al., 1987; Zöller and Wagner, 1990; Frechen et al., 1997; Novothny et al., 2009; Újvári et al., 2014a; Thiel et al., 2014) has low  $\chi$  values at Paks (Pécsi, 1995; Pécsi et al., 1995; Sartori et al., 1999; Sartori, 2000). The intercalated loess accumulation horizon is well-developed, genetically regarded to be part of the soil Mf1. As a result of erosion, these soils are missing in a large part of the Paks Brickyard section, recorded in the profiles of Újvári et al. (2014a) and Thiel et al. (2014) as well. This latter work confirmed the presence of this hiatus using pIRIR290 ages (Supplementary Fig. 5). The underlying loess horizon was effected by erosion too (Pécsi et al., 1995; Sartori, 2000; Thiel et al., 2014). Whereas the corresponding U2-S1 pedocomplex is well-developed with the highest  $\chi$  value of  $170 \cdot 10^{-8} \text{m}^3 \text{kg}^{-1}$  recorded in the lower member of the profile (U2-S1S2).

While there are two weakly developed paleosols in the uppermost 5 m of the Udvar profile (U2-L1S1, U2-L1S2), in case of Paks we come across structured fine sandy loess (L1) with thin fine sand intercalations between the depths of 3–5 m, corresponding to layered slope erosional infillings (Dell 1 and Dell 2) (Fig. 6). These two erosional horizons were also recorded by Thiel et al. (2014) although at a higher position. Thiel et al. (2014) interpreted them as representing either soil erosional horizons or depressions characterized by higher accumulation rates due to enhanced erosion from the nearby geomorphological highs. The uppermost loess layer is divided from the next loess unit (L2) by a steppe embryonic soil (H) at 6 m.

According to our results, we may presume that the two sites followed similar evolutionary pathways from 800 to about 400 ka, when conditions changed. This assumption is justified on the similar thickness of the comparable loess and intercalated

paleosols on the one hand. On the other hand, similar  $\chi$  values also corroborate this statement. However, there is a marked change in paleosol positions, deposit thickness and upward trends observable in  $\chi$  values from 400 ka onwards (Fig. 6), right after the so-called Mid-Brunhes transition (An et al., 1990; Hovan et al., 1991; Ding et al., 2005; Sun et al., 2006; Lambert et al., 2012). Reasons behind the change are climatic and/or tectonic (Kretzoi and Krolopp, 1972; Marković et al., 2009; Sümeği and Gulyás, 2009; Varga, 2011; Varga et al., 2011; Buggle et al., 2013; Sümeği et al., 2012a; b).

## 5.2. Interprofile correlation with the Serbian sites of Stari Slankamen, Batajnica and Mošorin

In Vojvodina data from three sites (Stari Slankamen, Batajnica, Mošorin) have been used to establish a pan-European pedostratigraphic, lithostratigraphic system for the past ca. 1 Ma (Marković et al., 2015). The proposal was based on a composite profile created via stitching together the records of two out of the three referred sites: Stari Slankamen and Mošorin (Marković et al., 2015). The new composite profile was regarded as the stratotype of the Danubian Basin Pleistocene climatic and environmental evolution giving the backbone of inter- and extraregional correlation with Eurasian terrestrial other, ice-core and marine archives spanning the last one million years (Marković et al., 2015). For this purpose, a complex chronology was derived using comparative pedostratigraphies, lithostratigraphies, amino-acid chronologies, absolute luminescence chronologies complemented by visually observed and presumed marker tephra horizons most of which were not clearly dated. A limited amount of magnetostratigraphic measurements added further tiepoints to the referred chronology complemented by magnetic susceptibility as an ideal tool for interprofile correlation. In addition, orbital tuning was also attempted for refinement and reliability testing. The new composite profile was correlated with the long-known records of China, as well as other European records spanning the last 1 million years. Climatic cycles and megacycles have also been identified and interpreted using the synthesis profile (Marković et al., 2015). However, the accuracy of the newly proposed chronostratigraphic, pedo- and lithostratigraphic system depends on the fidelity of the inferred chronology limited by the precision of applied dating techniques.

Out of the three referred Serbian sites, Stari Slankamen is the only one where relatively detailed magnetostratigraphic work has been done (Hambach et al., 2009; Marković et al., 2011) (Fig. 7). Nevertheless, it was confined to the bottom part of the profile yielding two independent geomagnetic reversals within the Brunhes chron suitable for chronological correlation. Namely, the MBB below the V-S8 pedocomplex and the Stage 17 excursion above the V-S6 pedocomplex (Hambach et al., 2009; Marković et al., 2011, 2012a,b; 2015). So, age-tie points related to the MBB, Stage 17 excursion could be accepted as reference for building an independent absolute chronology. In addition, pIRIR290 luminescence ages down to V-L3 (>230 ka) corresponding to MIS 8 are reliable and of further use. AAR relative stratigraphy yielded good results down to MIS 8, but as was highlighted in our paper earlier results beyond MIS 8 are not fully consistent and acceptable in our view.

In Batajnica, found ca. 30 km north of Stari Slankamen, only the lowermost 6 m have been investigated using paleomag dating techniques alone stating the presence of normal polarities, thus reinforcing the age of the entire profile to be within the Brunhes chron (Marković et al., 2009, 2011; 2012a,b, 2015). No further geomagnetic reversals were recorded hampering a more exact position of the profile within the presently accepted system of GITS.

Presence of tephras have been postulated for Batajnica and the nearby site of Ruma ca. 20 kms to the west in the V-L2 horizon representing MIS 6 (Marković et al., 2008, 2009; 2012a,b, 2015). This assumption was based on a small peak at a depth of ca. 13 m in the former and ca. 10 m in the latter site (Fig. 7). Compared to magnetic susceptibility values recorded for over- and underlying paleosols there is no major difference, which can actually question the existence of these hypothetical cryptotephra horizons in the lack of geochemical and chronological data. The upper tephra in V-L2 (Fig. 7) was hypothetically correlated with the tephra of the Gorjanović profile in Osijek, Croatia (Marković et al., 2012a,b, 2015), having a similar stratigraphic position and a minimum luminescence age of 145 ka (Wacha and Frechen, 2011; Wacha et al., 2013) which is in line with the proposed MIS 6 age of V-L2. At the top of V-S5, at a depth of ca. 30 m, the presence of another cryptotephra was postulated for the site of Batajnica (Marković et al., 2012a,b, 2015). This cryptotephra was correlated with another cryptotephra postulated for the lowermost part of the Mošorin profile sitting on top of the lowermost V-S5 paleosol (Fig. 7) again on the basis of observed MS peaks. However, these are almost equally weak as in case of the V-L2 tephtras.

In Mošorin, ca. 30 km north of Stari Slankamen, apart from the inferred and later visually corroborated upper tephra horizon in V-L2, which was potentially correlated with the Gorjanović profile tephra having minimum luminescence age of 142 ka (Marković et al., 2012a,b, 2015), not much gives a reliable starting point for building an independent chronology (Fig. 7). The lower assumed tephra marked by an MS peak at the depth of 36 m on top of V-S4 in the Mošorin profile was tephrostratigraphically equated with the Bag Tephra (Marković et al., 2012a,b) recorded in several profiles in Hungary (Basaharc, Dunaszekcső, Mórág, Paks etc. (Sümegei, 1991; Hum and Sümegei, 2000, 2001; Horváth, 2001; Hum, 2002, 2005; 2007; Sümegei and Krolopp, 2005, 2006; Újvári et al., 2014a; Thiel et al., 2014) having an age placed between 360 and 410 ka (Figs. 7–8). The assumed presence of another tephra horizon on the top part of V-S5 may be another pillar, but its age is only tentative in the lack of geochemical and chronological data. Marković et al. (2015), marking this as the S5 cryptotephra, presents an approximate age of ca. 500 ka though. Based on the general stratigraphic position of V-S5 and a presumption presented in several works the V-S5 paleosol was correlated with the S5 paleosol of Chinese LPSs representing MIS 13–15 (Marković et al., 2008, 2009, 2011, 2012a,b, 2015; Fitzsimmons et al., 2012). The referred presumption was based on the generally well-developed nature of V-S5 similarly to its Chinese counterpart in addition to highly similar MS patterns. So, the age of the S5 cryptotephra is postulated on the basis of its stratigraphic position rendering its reliability highly ambiguous.

Fig. 7 presents the results of interprofile correlation between our study site of Udvari-2A and those of the referred Serbian sites. The weakly developed MIS 3 paleosols U2-L1S1 and U2-L1S2 is correlated with the V-L1S1, V-L1-S2 and V-L1S3 paleosol horizons of Stari Slankamen. From  $^{14}\text{C}$  data bracketing the two MIS 3 paleosols at Udvari-2A the upper one ( $24.8 \pm 0.174$  ka cal BP) is clearly comparable with pIRIR290 age of Murray et al. (2014) recorded above the V-L1S1 paleosol ( $23.6 \pm 1.4$  ka) corroborating the accuracy of our correlation. Loess (V-L2) under the V-S1 paleosol at Stari Slankamen yielded pIRIR290 age of  $170 \pm 13$  ka (Murray et al., 2014), which is comparable with the age of our recorded Iceland Basin geomagnetic excursion (191 ka) in U2-L2 corroborated by the uppermost occurrence of our biostratigraphic marker gastropod. The MIS 7 paleosol is eroded at Stari Slankamen confirmed by visual observations made on the field (Marković et al., 2011). However, there is a minor discrepancy regarding the placement of the erosional level (EL) and the nomenclature of the overlying interstadial paleosol. The original description of Marković et al. (2011)

puts it to the depth of 13 m, which is adopted by the latest chronostratigraphic work of Murray et al. (2014). In line with this interpretation the overlying eroded paleosol is named V-L2S1. In their most recent publication, Marković et al. (2015) presents the EL at the same depth on Fig. 4. But on Fig. 8 presenting the results of luminescence dating and AAR relative chronology the EL is moved upward above the originally referred V-L2S1 paleosol, which is then altered to V-L3S1. Despite this unexplained confusion, the MIS 7 correspondence of this horizon is quite straightforward in the light of relative AAR chronology and pIRIR290 age of the underlying loess with minimal age estimate of  $>230$  ka. Loess units between V-S3 and V-S4 and below (V-L5) yielded pIRIR290 ages  $>330$  ka and  $>350$  ka, respectively. Although the signal reaches saturation around 300 ka (Thiel et al., 2011, 2014; Murray et al., 2014) and these can be regarded as minimal ages only, estimates are remarkably in line with our understanding of the correlation of the V-S3 and V-S4 units with the U2-S3 pedocomplex bracketed by the MIS 8 and MIS 9 occurrences of the biostratigraphic marker *Neostyriaca corynodes*. (Fig. 7). The pedocomplex of U2-S3 in Udvari is composed of an upper member with well developed B and Bw horizons (b3B, b3Bw) separated by a zone of carbonate accumulation (b3Bkn) from the lower member of a similarly well-developed B horizon (b3B2). V-S3 is made up of an Ah and A horizon according to the pedological description (Marković et al., 2011) separated by a thin loess horizon of 330 ka minimum age from the underlying V-S4 paleosol having a relatively well developed B horizon. These pedological features on their own would hint to the unification of V-S3 and V-S4 as a single pedocomplex (V-S3) corresponding to MIS 9. Minimum ages bracketing this pedocomplex ( $>230$  ka and  $>350$  ka) and the intervening thin loess ( $>330$  ka) are not only getting older with the stratigraphy but are also in line with our accepted ages for MIS 10 and MIS 8, implying that the pedocomplex in between is in fact representing MIS 9. This remarkable correspondence may also presume that conditions might have favored a higher saturation of the pIRIR290 signal and minimum ages are in fact acceptable. The total thickness of this new composite pedocomplex is also comparable with that of the U2-S3 pedocomplex corresponding to MIS 9 (Fig. 7). Beyond this unit pIRIR290 ages are reversed and clearly yield unreliable results (Murray et al., 2014) hampering the accurate chronological assignment of the underlying paleosol marked as V-S5, having a well-developed rubified Bw horizon and the succeeding embryonic soil (V-L6S1). The next reliable control point at Stari Slankamen is the Stage 17 excursion above V-S6, recorded in a similar stratigraphic position at Udvari-2A above U2-S6, clearly assigning this paleosol to MIS 17. In addition, both have a well-developed carbonate accumulation zone (b6Bc) below a B (b6B) or Bw horizon, respectively. The recorded and reconsidered position of the MBB between the V-S7 and V-S8 pedocomplex, as well as the U2-S7 and U2-S8 pedocomplexes at Udvari-2A clearly assigns this unit to MIS 19 and MIS 21 respectively. V-S9 may form a part of the MIS 21 pedocomplex putting the lowermost welded basal complex at Stari Slankamen to MIS 23 and beyond, similarly to the top part of the corresponding U2-S9 paleosol. Turning back to the question of the remaining well-developed V-S5 and embryonic V-L6S1 paleosols the only reliable information that we have at Stari Slankamen is that they are younger than MIS 17, but definitely older than MIS 8. On the basis of our previously mentioned statements, the V-S5 pedocomplex is correlated with our U2-S4 pedocomplex assigned to the longest interglacial MIS 11. This would place the embryonic soil V-L6S1 to MIS 13–15 also represented by weak paleosols at Udvari (U2-S5) and sandy, clayey hydromorphic soils at Paks (Mtp1+2, Phe). Problems surrounding disparities regarding the assignment of V-S5 paleosols in Vojvodina and S5 paleosols in Bulgaria and Romania as well as the referred Mtp1+2, Phe pedocomplex to MIS 13–15 are to

be discussed in the next section rendering further support for our correlation of the V-S5 paleosol with MIS 11.

Correlation of loess/paleosol units down to MIS 8 at Batajnica with the two previous sites is relatively straightforward, despite the fact that there is only a single control point of a presumed tephra in V-L2 with an assumed age of 142 ka marking MIS 6. The paleosol V-S2 is clearly correlated with our U2-S2 paleosol both representing MIS 7. V-S3 and V-S4 at Batajnica has similar MS values to V-S3 and V-S4 at Stari Slankamen the latter being weaker. Due to this similarity and what has been stated about these paleosols at Stari Slankamen we are again proposing the unification of the two paleosols into a single pedocomplex corresponding to MIS 9. This assumption is further corroborated when we look at the profile for Mošorin. The MS pattern of the V-S3 paleosol correlated with MIS 9 there displays a similar trend to the one mentioned about the united paleosols of V-S3 and V-S4 at Batajnica and Stari Slankamen. If the pronounced MS peak above the V-S4 paleosol at Mošorin clearly representing a tephra truly corresponds to the Bag Tephra, then the age of the V-L4 loess there is securely MIS 10. On the other hand, it would ultimately mean that the S5 cryptotephra at Batajnica should be correlated with the mentioned middle tephra horizon above V-S4 at Mošorin. This seems reasonable considering the stratigraphic position of the two tephra and the similar MS patterns of the referred corresponding paleosols (Fig. 7). Returning to the lowermost part of Batajnica, based on similar stratigraphic position and MS shapes, the lowermost unnamed pedocomplex unit can be reasonably correlated with the MIS 17 pedocomplexes of Stari Slankamen and Udvari-2A. Using this logic and the assigned MIS 11 age of the V-S4 paleosol at Mošorin the corresponding V-S5 complex in that profile should also be placed into MIS 17. So, the intervening part should represent MIS 13–15 in both profiles. It's interesting to note that the shape of the MS curve between V-S5 and the lowermost unit between the depths of 37–40 m is very similar to the one at Paks, where the minor wiggles could have been assigned to sandy and clayey hydromorphic paleosols (Mtp1+2, Phe) corresponding to MIS 13–15. In addition, this whole pedocomplex below V-S5 at Batajnica displays increasing hydromorphic characteristics similarly to our MIS 13–15 paleosols at Paks and Udvari-2A.

## 6. Discussion

### 6.1. A revised correlation scheme for DBPLs from MIS 1 to MIS 31

From the regional profiles of the Middle Danube Basin only the Hungarian site Udvari 2A has relatively high-resolution independent absolute chronology for the past ca. 1100 ka, which is primarily based on multiple recorded paleomagnetic excursions within the Brunhes and Matuyama chrons,  $^{14}\text{C}$  dates, all underpinned by independent biostratigraphic control and tephrochronology.

In the other referred Hungarian, Serbian, Romanian, Bulgarian profiles the only control point within the Brunhes chron was the position of the MBB in general (Pécsi and Pevzner, 1974; Pécsi, 1995; Pécsi et al., 1995; Jordanova and Petersen, 1999; Sartori, 2000; Panaiotu et al., 2001; Jordanova et al., 2007, 2008; Marković et al., 2011, 2012a,b; 2015; Fitzsimmons et al., 2012; Rădan, 2012). The MBB in Hungary was only recorded at Paks, Dunaszekcső (Márton, 1979; Pécsi and Pevzner, 1974) and some borehole profiles in SE Transdanubia (Marsi et al., 2004) in addition to Udvari-2A (Márton, 1998). From the numerous Vojvodinian profiles mentioned, the MBB was recorded at Stari Slankamen alone (Hambach et al., 2009; Marković et al., 2011, 2012a,b; 2015). Besides the MBB, the stage 17 excursion was also recorded here, just like in the borehole sequence of Udvari-2A (Hambach et al., 2009; Marković et al., 2011, 2012a,b; 2015). pIRIR290 luminescence dating could confirm the absolute

age of loess/paleosol units down to ca 300 ka (MIS 9) only at two sites: Paks and Stari Slankamen (Murray et al., 2014; Thiel et al., 2014; Marković et al., 2015). Correlation of loess/paleosol units between MIS 10 and MIS17 was thus rather tentative both in these two referred sites and additional ones from Vojvodina, Bulgaria and Romania. Consequently, the record of Udvari-2A is suitable to revise established chronostratigraphies of the Middle and Lower Danube Basin LPSs.

Fig. 8 presents a new interprofile correlation of DBLPSs based on the chronology of the LPS of Udvari-2A discussed in this work. Correlations between S1 and S2 paleosols corresponding to MIS 5 and MIS 7 presented in the scheme of Marković et al. (2015) was accepted. S3 and S4 paleosols were originally assigned to MIS 9 and MIS 11 at Stari Slankamen, Batajnica and in the composite profile for Vojvodina as well (Marković et al., 2015). Based on our record for MIS 9 (U2-S3) S3 and S4 at these sites were merged into a single pedocomplex. It's interesting to note that the new S3 pedocomplex is a double one in all Serbian sites except Mošorin. In Udvar-2A the U2-S3 unit is likewise composed of two subunits (U2-S3S1 and U2S3S2). The other Hungarian site of Paks is an outlier similarly to Mošorin. In addition, the lower member of the new S3 pedocomplex (formerly designated as S4) is generally characterized by lower magnetic susceptibility values compared to the upper one. This observation is valid for all Serbian, Romanian and Bulgarian sites except Viatovo, where values of the two peaks are almost identical (Supplementary Fig. 6). It may be worth nothing that in the first publication on the LPS of Ruma (Marković et al., 2006), only three paleosols are recorded, which were accurately correlated with MIS 9. However, in later publications the lower peak is designated as V-S4 without any detailed explanation for the reason of the change and is reclassified with MIS 11 (Marković et al., 2009, 2011 2012a,b, 2015). As new coeval Vojvodina sites were introduced in the referred new publications, there is every reason to believe that the initial pedostratigraphy for Ruma was altered in light of the similarities of magnetic susceptibility curves for V-S3 and V-S4 paleosols at Batajnica and Stari Slankamen. S3 and S4 was also merged for the Bulgarian sites of Koriten and Viatovo as well as the Romanian site Zimnicea giving S3 assigned to MIS 3. In case of Mostistea and Mircea Voda in Romania the formerly determined S3 horizons were accepted to correspond to MIS 9 (Fig. 8).

Merging of S3 and S4 paleosols into a new S3 at the referred sites depicted on Fig. 8 had a serious consequence on the formerly proposed age and chronostratigraphic importance of the pedocomplex originally designated as V-S5 or S5 in Serbia, Romania and Bulgaria. The position of S5 was determined on a pure pedostratigraphic basis for all Vojvodinian, Romanian and Bulgarian sites in the lack of reliable chronological data. Former studies correlated the pedocomplexes PK7+8 in the Czech Republik, Phe and Mtp1+2 in Hungary, V-S5 in Serbia and S5 in Romania and Bulgaria with the S5 (MIS 13–15) pedocomplex of the Chinese loess plateau (Marković et al., 2009, 2011; 2012a,b, 2015; Fitzsimmons et al., 2012). It was based on an assumed presence of a uniform stratigraphic marker horizon of MIS 13–15 linking Chinese and European stratigraphies. The proposal of this horizon is rooted in the assumption, that if MIS 13–15 deposits represented by the S5 soil in Chinese LPSs are well-developed (Porter, 2001, 2007; Nutgeren et al., 2004; Hao and Guo, 2005; Yin and Guo, 2006, 2008; Yin et al., 2008; Guo et al., 2009a; b; Sun et al., 2009; Hao et al., 2012; Yin and Berger, 2012), then there must be an interglacial in Europe as well, whose deposits' characteristics are comparable with those of the S5 soil in China (Bronger and Heinkele, 1989; Bronger et al., 1998; Vandenberghe, 2000; Bronger, 2003). This assumption was further reinforced by the general presence of a well-developed, clay-rich paleosol considered to represent S5 in DBLPSs. The best was given by the Polish deposits corresponding to

the so-called Ferdynandovian interglacial. According to Vandenberghe (2000), the Ferdynandovian interglacial represents a long complex warm period, which is separated by a glacial from the succeeding Holsteinian interglacial (base of S4 in China; i.e. MIS 11) based on litho-pedostratigraphical observations in Poland. The Ferdynandovian interglacial was taken to be coeval with the Cromerian IV in Northwestern European stratigraphy (Vandenberghe, 2000). Cromerian IV deposits in the Netherlands contain augite remains, which were equated with the Riedener Phase of Eifel volcanism in NW Germany (Zagwijn, 1985) dated between 350 and 450 ka (Van den Boogaard and Schminke, 1990; Boenigk and Frechen, 1998). As Holsteinian deposits are overlying the Cromerian IV ones, Zagwijn (1996) equated Cromerian IV corresponding to the Ferdynandovian interglacial with MIS 11 not MIS 13, and the Holsteinian with MIS 9. Cromerian IV deposits at the Eifel site of Kärlich are overlain by loess developed under permafrost conditions bearing Riedener Phase tephra dated between 350 and 450 ka. Based on the most recent LR04 benthic stack of Lisiecki and Raymo (2005), the loess over the Cromerian IV deposits at this German site should correspond then to MIS 10. Vandenberghe (2000) notes that pre-Cromerian IV deposits are augite-bearing too (Razi Rad, 1976), implying that tephra accumulation must have started earlier than 450 ka; i. e. during MIS 12. So, he equates the cold loess deposits at Kärlich with MIS 12. This concept corroborates him in his previous assumption that the Cromerian IV and the corresponding Ferdynandovian interglacial should in fact be correlated with MIS 13 and S5 in China (Vandenberghe, 2000). According to our view, field observations made at Kärlich can not exclude the possibility of two different tephra accumulation events connected to the Riedener Phase volcanism dated between 350 and 450 ka. Evidence of similar multiphase accumulations of the Bag Tephra equated with MIS 10 was noted in some SE Transdanubian sites in Hungary (Hum and Sümeği, 2000, 2001; Hum, 2002, 2005, 2007). Based on the stratigraphical position of the referred tephra layers and the available range of absolute age we may presume that the Cromerian IV deposits at Kärlich are clearly bracketed by

tephras of MIS 10 and MIS 12 age confirming the conclusion of Zagwijn (1996). Based on this, the stratigraphic marker horizon of MIS 13–15 of Vandenberghe (2000) for NW Europe can be refuted. So, the S5 pedocomplexes at Vojvodinian, Romanian and Bulgarian sites should be reassigned to MIS 11. Reassignment to one of the best developed and longest interglacials of the past 800 ka; MIS 11 better explains the generally observed higher degree of pedogenesis in case of these pedocomplexes.

Conversely, the age of S5 pedocomplexes at the Hungarian sites of Udvari-2 A and Paks is verified by bracketing ages of pedocomplexes representing MIS 11 and MIS 16. However, in contrast to other DBLPSs, these are weakly developed and affected by hydro-morphic features in their lower parts. The weak development of MIS 13–15 pedocomplexes observed in the referred Hungarian sites is more in line with low magnitude climate cycles characteristic of the Early Middle Pleistocene before the Mid-Brunhes transition. The best expression of these low-magnitude climate cycles is in MIS 13, which is routinely the coolest interglacial of the past 800, 000 years in various long palaeoenvironmental records from around the world (Lang and Wolff, 2011; Candy and McClymont, 2013). MIS 13 is characterized by lower greenhouse gas (CO<sub>2</sub>, CH<sub>4</sub>) concentrations (Louergue et al., 2008; Lüthi et al., 2008; Yin and Berger, 2012), cool Antarctic temperatures (Jouzel et al., 2007) and high benthic δ<sup>18</sup>O values (Lisiecki and Raymo, 2005; Raymo et al., 2006) related to higher global ice-volume and/or colder deep ocean temperatures. Insolation values however were not abnormal compared to other interglacials (Lang and Wolff, 2011). In Chinese LPs a strong MIS 13–15 interglacial is hallmarked by a well-developed S5 pedocomplex (Porter, 2001, 2007; Bronger, 2003; Nutgeren et al., 2004; Hao and Guo, 2005; Yin and Guo, 2006, 2008, 2008; Yin et al., 2008; Guo et al., 2002, 2009a; b; Sun et al., 2009; Hao et al., 2012; Yin and Berger, 2012), because of an enhanced East-Asian Summer Monsoon (EASM) bringing more precipitation. MIS-13 though has a larger eccentricity and its NH summer occurred at perihelion, which leads to a higher summer insolation in the Northern Hemisphere. This leads to the presence

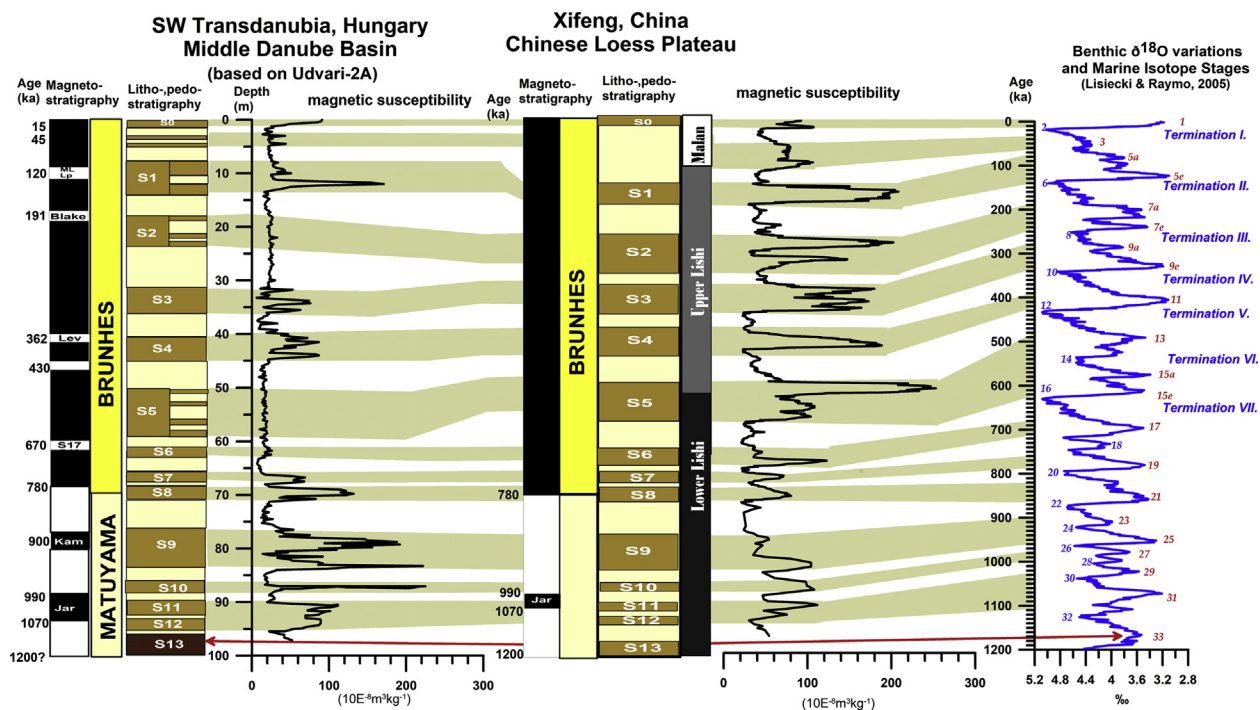


Fig. 9. New ideal stratigraphic column for the past 1.1 Myr for SW Transdanubia, Hungary compared to the Chinese loess/paleosol sequence of Xifeng.

of Eurasian ice sheet controlled climates of both the northern Atlantic and China too (Yin et al., 2008; Lang and Wolff, 2011; Candy and McClymont, 2013). The climatic setting of Europe during MIS 13 characterized by weaker latitudinal temperature gradients across NW and SW Europe was significantly different from that seen in later interglacials. Longitudinal climate gradients on the other hand were much stronger (Candy et al., 2010, 2015; Candy and McClymont, 2013). This paleoclimatic disparity needs to be carefully considered when discussing climatic conditions, seasonality and soil development for the DBLPSs in context of those recorded for Central and SE Asia. As S6 in Vojvodina and U2-S6 in Hungary can be securely correlated with MIS 17 based on independent magnetostratigraphic data (S17 excursion), coeval S6 horizons in Romania (Zimnicea) and Bulgaria (Koriten, Viatovo) must equally represent this stage (Fig. 8) This is further corroborated by the presence of the MBB in all referred sites of Viatovo, Koriten and Zimnicea as a control point. Horizons located between the VS5 and V-S6 units in Stari Slankamen and Batajnica, which were assigned to MIS 11 and MIS 17 per our new results, are characterized by low MS values (Supplementary Fig. 6) comparable to those recorded for the U2-S5 pedocomplex at Udvari-2A and the S5 pedocomplex of Paks (Hs1, Mtp 1 + 2, Phe 2) assigned to MIS 13–15. In Batajnica increasing hydromorphic influence is noted downwards from the top of the originally established V-S5 pedocomplex with higher intensities below the referred paleosol (Fig. 7). Similar observations were made in the lower part of the U2-S5 pedocomplex of Udvari-2A and S5 pedocomplex of Paks (Hs1, Mtp 1 + 2, Phe 2) implying the emergence of comparable climatic and environmental conditions during the formation of these pedocomplexes.

### 6.2. Correlation of an ideal stratigraphic column for SW Transdanubia, Hungary with the LPS of Xifeng, China

As seen in the previous sections so far the Hungarian LPS of borehole Udvari-2A seems to be the best resolved, thickest Quaternary sequence in the Carpathian Basin with reliable absolute chronology. This called for the construction of an ideal stratigraphic column for the area of SW Transdanubia, which may serve as a basis of future regional and extraregional correlations dating back 1.1 Ma (Fig. 9). In this ideal profile all paleosols from S1 to S13 correspond to S1-S13 paleosols of the Xifeng profile in the Chinese loess plateau. Within the Matuyama chron the S11 and S12 paleosols were correlated with MIS 29–MIS31 supported by the position of the Jaramillo subchron as well. S10 just above the Jaramillo suchron thus must represent MIS 27. In light of this information the lowermost pedocomplex of S13 should be correlated with MIS 33. S9 is characterized by a double MS peak in both profiles. The upper peak is bracketed by the Kamikatsura excursion, which automatically assigns this part to MIS 23. The lower part of S9 thus might correspond to MIS 25. Within the Brunhes chron S1 was assigned to MIS5, S2 to MIS 7, S3 to MIS 9. It's interesting to note three peaks on the MS curves of both profiles implying the presence of all stadials and interstadials within this interglacial recorded in the marine isotope curve too from MIS 9a to 9e. S4 was correlated with MIS 11, while S5 with MIS 13–15. In our profile the S5 pedocomplex is composed of 4 weakly developed soils, which could correspond to the substages of MIS13 and MIS 15. S6 represent the MIS 17 interglacial, while S7 and S8 are correlated with MIS 19 and MIS 21. Finally, it might be worth noting that while there is an upward increase in MS values of the Chinese profile, an opposite trend is seen for the Hungarian one from MIS 31. In Xifeng the MS values are in the same ranges around  $100 \cdot 10^{-8} \text{m}^3 \text{kg}^{-1}$  up to about the bottom part of S5 corresponding to MIS 15. In the Hungarian profile the S12 and S11 paleosols have similar MS values to the same paleosols in China. In the Hungarian profile the S10 and S9 pedocomplexes are

characterized by the highest MS values of the entire profile, which is ca. double of that of the underlying paleosols and the corresponding Chinese paleosols. Yet the general trend up to the Brunhes-Matuyama boundary appears to be the same. From the MBB there is a general gradual upward decrease in MS values in Hungary with major fluctuations plus the exception of the MIS 5 pedocomplex. In China this period is characterized by an upward increase in MS values. Elucidating the reasons for these differences and making inferences regarding paleoenvironmental evolution of the sites is the subject of further studies.

## 7. Concluding remarks

The presence of geomagnetic control points at and near the MBB confirms the fidelity of the proposed pan-European stratigraphic correlation scheme presented in Marković et al. (2015) for the interval between MIS 17–21. Conversely, the refusal of the MIS 13–15 stratigraphic marker horizon and the merging of paleosols S3 and S4 is a major blow on the chrono- and pedostratigraphy presented for MIS 9–MIS 17 in this scheme. There is an important moral of the story presented. It's high time we abandon our strict reliance on pedostratigraphy and lithostratigraphy in correlation and the method of simple wiggle matching without reliable, multiple cross-validated independent chronostratigraphic data. An almost perfect match of these features is a nuisance, clearly incompatible with our understanding the functioning of our Earth System. Instead, it leads to grandiose a priori assumptions, which significantly bias our workflow, and interpretations yielding unreliable results and conclusions. A good example was how the ultimate belief in the existence of a stratigraphic marker horizon (MIS 13–15), which was based on the mentioned similarities in pedology and lithology without age control, plus its strong bias by features observed at internationally highly acknowledged sites (well-developed S5 paleosols in Chinese loess/paleosol sequence) astray objective evaluations and further conclusions made on nature and temporal aspects of climatic cycles and supercycles.

## Acknowledgements

The research was supported by the European Union and the State of Hungary, co-financed by the gs1:European Regional Development Fund in the project of GINOP-2.3.2-15-2016-00009 'ICER'. We are grateful for the two anonymous reviewers whose comments helped improving the content of the manuscript to its present form.

## Appendix A. Supplementary data

Supplementary data related to this article can be found at <https://doi.org/10.1016/j.quascirev.2018.04.012>.

## References

- Landscape Geography of Hungary. In: Ádám, L., Marosi, S., Szilárd, J. (Eds.), 1981. Magyarország tájféldrajza IV. A dunántúli-dombság (Dél-Dunántúl), vol. 4. The Transdanubian Hills (South Transdanubia), Akadémiai Kiadó, Budapest. in Hungarian).
- An, Z., 2000. The history and variability of the East Asian paleomonsoon climate. *Quat. Sci. Rev.* 19, 171–187.
- An, Z., Liu, T., Lu, Y., Porter, S.C., Kukla, G., Wu, X., Hua, Y., 1990. The long-term paleomonsoon variation recorded by the loess-paleosol sequence in Central China. *Quat. Int.* 7–8, 91–95.
- Ankjaergaard, C., Guralnik, B., Buylaert, J.-P., Reimann, T., Yi, S.W., Wallinga, J., 2016. Violet stimulated luminescence dating of quartz from Luochuan (Chinese loess plateau): agreement with independent chronology up to ~600 ka. *Quat. Geoch.* 34, 33–46.
- Banerjee, S.K., Jackson, M., 1996. Wind-borne dust holds clues to early climate. *Earth Space* 8, 12–14.

- Barnett, T.P., Schlesinger, M.E., 1987. Detecting changes in global climate induced by greenhouse gases. *J. Geophys. Res.* 92, 14772–14780.
- Basarin, B., Buggle, B., Hambach, U., Marković, S.B., O'Hara-Dhand, K., Kovačević, A., Stevens, T., Guo, Z.T., Lukić, T., 2014. Time-scale and astronomical forcing of Serbian loess–paleosol sequences. *Glob. Planet. Chang.* 122, 89–106.
- Biswas, D.K., Hyodo, M., Taniguchi, Y., Kaneko, M., Katoh, S., Sato, H., Kinugasa, Y., Mizuno, K., 1999. Magnetostratigraphy of Plio-Pleistocene sediments in a 1700-m core from Osaka Bay, southwestern Japan and short geomagnetic events in the middle Matuyama and early Brunhes chrons. *Palaeogeogr. Palaeoclim.* 148, 233–248.
- Boenigk, W., Frechen, M., 1998. Zur Geologie der Deckschichten von Kärlich/Mittelrhein. *Eiszeitalt. Ggw.* 48, 38–49.
- Borsy, Z., Felszerfalvy, J., Szabo, P.P., 1979. Thermo-luminescence dating of several layers of loess sequences at Paks and Mende (Hungary). *Acta Geol. Acad. Sci. Hung.* 22, 451–459.
- Braconnot, P., Harrison, S.P., Kageyama, M., Bartlein, P.J., Masson-Delmotte, V., Abe-Ouchi, A., Otto-Bliesner, B., Zhao, Y., 2012. Evaluation of climate models using palaeoclimatic data. *Nat. Clim. Change* 2, 417–424.
- Broecker, W.S., 1987. Unpleasant surprises in the greenhouse? *Nature* 328, 123–126.
- Bronger, A., 2003. Correlation of loess–paleosol sequences in East and Central Asia with SE Central Europe—towards a continental Quaternary pedomorphology and paleoclimatic history. *Quat. Int.* 106 (107), 11–31.
- Bronger, A., Heinkele, T., 1989. Micromorphology and genesis of paleosols in the Luochuan loess section, China: pedomorphological and environmental implications. *Geoderma* 45, 123–143.
- Bronger, A., Winter, R., Sedov, S., 1998. Weathering and clay mineral formation in two Holocene soils and in buried paleosols in Tajikistan towards a Quaternary paleoclimatic record in Central Asia. *Catena* 34, 19–34.
- Bronk Ramsey, C., 2009. Bayesian analysis of radiocarbon dates. *Radiocarbon* 51, 337–360.
- Brown, N.D., Forman, S.L., 2012. Evaluating a SAR TT-OSL protocol for dating fine-grained quartz within Late Pleistocene loess deposits in the Missouri and Mississippi river valleys. *United States. Quat. Geochron.* 12, 87–97.
- Brunnacker, K., Jánosy, D., Krolopp, E., Skoflek, I., Urban, B., 1980. Das jungmittelpleistozäne Profil von Süttö 6 (Westungarn). *Eiseltalter Ggw.* 30, 1–18.
- Bucsi-Szabó, L., Drahos, D., Lendvay, P., Szongoth, G., Zilahi Sebess, L., 1997. Well-logging investigations in the boreholes Úveghuta-1, Udvari-2 and Diósberey-1. *Ann. Rep. Geol. Inst. Hung.* 1996/II, 307–315.
- Buggle, B., Hambach, U., Glaser, B., Gerasimenko, N., Marković, S.B., Glaser, I., Zöller, L., 2009. Magnetic susceptibility stratigraphy and spatial and temporal paleoclimatic trends in East European loess paleosol sequences. *Quat. Int.* 196, 86–106.
- Buggle, B., Hambach, U., Kehl, M., Marković, S.B., Zöller, L., Glaser, B., 2013. The progressive evolution of a continental climate in SE-Central European lowlands during the Middle Pleistocene recorded in loess paleosol sequences. *Geology* 41, 771–774.
- Butrym, J., Maruszczak, H., 1984. Thermoluminescence chronology of younger and older loesses. In: Pecs, M. (Ed.), *Lithology and Stratigraphy of Loesses and Paleosols*. Hung. Acad. Sci., Budapest, pp. 195–199.
- Candy, I., McClymont, E.L., 2013. Interglacial intensity in the North Atlantic over the last 800,000 years: investigating the complexity of the mid-Brunhes Event. *J. Quat. Sci.* 28, 343–348.
- Candy, I., Coope, G.R., Lee, J.R., et al., 2010. Pronounced warmth during early middle pleistocene interglacials: investigating the mid-Brunhes event in the British terrestrial sequence. *Earth-Science Rev.* 103, 183–196.
- Candy, I., Schreve, D., White, T.S., 2015. MIS 13–12 in Britain and the North Atlantic: understanding the paleoclimatic context of the earliest Acheulean. *J. Quat. Sci.* 30, 593–609.
- Channel, J.E.T., Raymo, M.E., 2003. Paleomagnetic record at ODP site 980 (Feni Drift, Rockall) for the past 1.2 Myrs. *Geochem. Geophys. Geosystems* 4 (4), 1033.
- Channell, J.E.T., Hodell, D.A., Singer, B.S., Xuan, C., 2010. Reconciling astrochronological and Ar/Ar ages for the Matuyama–Brunhes boundary and late Matuyama chron. *Geochem. Geophys. Geosyst.* 11, 1–21.
- Chaput, M.S., Roberts, H.M., Duller, G.A.T., Lai, Z.P., 2016. Natural and laboratory TT-OSL dose response curves: testing the lifetime of the TT-OSL signal in nature. *Radiat. Meas.* 85, 41–50.
- Chlachula, J., Rutter, N.W., Evans, M.E., 1997. A late Quaternary loess–paleosol record at Kurtak, southern Siberia. *Can. J. Earth Sci.* 34, 679–686.
- Chlachula, J., Evans, M.E., Rutter, N.W., 1998. A magnetic investigation of a late Quaternary loess/paleosol record in Siberia. *Geophys. J. Int.* 132, 399–404.
- Cohen, K.M., Gibbard, P., 2016. Global Chronostratigraphical Correlation Table for the Last 2.7 Million Years. Subcommission on Quaternary Stratigraphy. International Commission on Stratigraphy, Cambridge, England.
- Crowhurst, S.J., 2002. Composite Isotope Sequence. The Delphi Project. <http://www.esc.cam.ac.uk/new/v10/research/institutes/godwin/body.html>.
- de Vernal, A., Hillaire-Marcel, C., 2008. Natural variability of Greenland climate, vegetation, and ice volume during the past million years. *Science* 320, 1622–1625.
- Davies, J.C., 2002. *Statistics and Data Analysis in Geology*. John Wiley and Sons, New York.
- Ding, Z.L., Derbyshire, E., Yang, S.L., Sun, J.M., Liu, T.S., 2005. Stepwise expansion of desert environment across northern China in the past 3.5 Ma and implications for monsoon evolution. *Earth Planet. Sci. Lett.* 237, 45–55.
- Fink, J., Kukla, G.J., 1977. Pleistocene climates in central Europe: at least 17 interglacials after the Olduvai event. *Quat. Res.* 7, 363–371.
- Fitzsimmons, K.E., Marković, S.B., Hambach, U., 2012. Pleistocene environmental dynamics recorded in the loess of the middle and lower Danube basin. *Quat. Sci. Rev.* 41, 104–118.
- Frechen, M., Horváth, E., Gábris, Gy., 1997. Geochronology of middle and upper pleistocene loess sections in Hungary. *Quat. Int.* 48, 291–312.
- Frechen, M., Oches, E.A., Kohfeld, K.E., 2003. Loess in Europe – mass accumulation rates during the last glacial period. *Quat. Sci. Rev.* 22, 1835–1857.
- Friedli, H., Lotscher, H., Oeschger, H., Siegentahler, U., Stauffer, B., 1986. Ice core record of the 13C/12C ratio of atmospheric CO<sub>2</sub> in the past two centuries. *Nature* 324, 237–238.
- Gábris, Gy., 2007. Kapcsolat a negyedidőszaki felszínalakító folyamatok időrendje és az oxigén-izotóp-rétegtan között a magyarországi lösz–paleotalaj-sorozatok és folyóvízi teraszok példáján (The relation between the time scale of the Quaternary surface processes and oxygen isotope stratigraphy according to the loess–paleosol sequences and river terraces in Hungary). *Földtani Közlemények* 137, 515–540.
- Guo, Z.T., Ruddiman, W.F., Hao, Q.Z., Wu, H.B., Qiao, Y.S., Zhu, R.X., Peng, S.Z., Wi, J.J., Yuan, B.Y., Liu, T.S., 2002. Onset of Asian desertification by 22 Myr ago inferred from loess deposits in China. *Nature* 416, 159–163.
- Guo, Z.T., Berger, A., Yin, Q.Z., Qin, L., 2009a. Strong asymmetry of hemispheric climates during MIS-13 inferred from correlating China loess and Antarctica ice records. *Clim. Past* 5, 21–31.
- Guo, Z.T., Berger, A., Yin, Q.Z., Qin, L., 2009b. Xifeng and Chanwu, China 800Kyr Loess Data. IGBP PAGES/World Data Center for Paleoclimatology Data Contribution Series # 2009-025. NOAA/NCDC Paleoclimatology Program. Boulder CO, USA.
- Guo, X.L., Liu, X.M., Lü, B., et al., 2011. Comparison of topsoil magnetic properties between the loess region in Tianshan Mountains and Loess Plateau, China, and its environmental significance (in Chinese). *Chin. J. Geophys.* 54, 1854–1862.
- Hambach, U., Zeeden, C., Hark, M., Zoeller, L., 2008. Magnetic dating of an upper Palaeolithic cultural layer bearing loess from the Krems–Wachtberg site (lower Austria). In: Reitner, J., et al. (Eds.), *Veränderter Lebensraum e Gestern, Heute und Morgen*. DEUQUA Symposium 2008, Abhandlungen der Geologischen Bundesanstalt, vol. 62, pp. 153–157.
- Hambach, U., Jovanović, M., Marković, S.B., Nowaczyk, N., Rolf, C., 2009. The Matuyama–Brunhes geomagnetic reversal in the Stari Slankamen loess section (Vojvodina, Serbia): its detailed record and its stratigraphic position. *Geophys. Res. Abstr.* 11, EGU2009–0.
- Hao, Q.Z., Guo, Z., 2005. Spatial variations of magnetic susceptibility of Chinese loess for the last 600 kyr: implications for monsoon evolution. *J. Geophys. Res.* Solid Earth 110. <https://doi.org/10.1029/2005JB003765>.
- Hao, Q.Z., Wang, L., Oldfield, F., Peng, S., Qin, L., Song, Y., Xu, B., Qiao, Y., Bloemendal, J., Guo, Z.T., 2012. Delayed build-up of Arctic ice sheets during 400,000-year minima in insolation variability. *Nature* 490, 393–396.
- Heil Jr., C.W., King, J.W., Zárate, M.A., et al., 2010. Climatic interpretation of a 1.9 Ma environmental magnetic record of loess deposition and soil formation in the central eastern Pampas of Buenos Aires, Argentina. *Quat. Sci. Rev.* 29, 2705–2718.
- Heller, F., Liu, T., 1982. Magnetostratigraphical dating of loess deposits in China. *Nature* 300, 431–433.
- Heller, F., Liu, T., 1984. Magnetism of Chinese loess deposits. *J. R. Astron. Soc.* 77, 125–141.
- Hertelendi, E., Sümeği, P., Szóór, Gy., 1992. Geochronologic and paleoclimatic characterization of quaternary sediments in the Great Hungarian plain. *Radiocarbon* 34, 833–839.
- Holden, P.B., Edwards, N.R., Wolff, E.W., Lang, N.J., Singarayer, J.S., Valdes, P.J., Stocker, T.F., 2010. Interhemispheric coupling, the west Antarctic ice sheet and warm Antarctic interglacials. *Clim. Past* 6, 431–443.
- Horváth, E., 2001. Marker horizons in the loess of the Carpathian Basin. *Quat. Int.* 76/77, 157–163.
- Horváth, E., Bradák, B., 2014. Sárga föld, lösz, lösz: short historical overview of loess research and lithostratigraphy in Hungary. *Quat. Int.* 319, 1–10.
- Horváth, E., Gábris, Gy., Juvigné, E., 1992. Egy pleisztocén vezérszint a Kárpát-medencében: a Bag Tefra (a marker in the pleistocene of the Carpathian Basin: the Bag tephra). *Földtani Közlemények* 122, 233–249.
- Hovan, S.A., Steven, A., Rea, A., David, K., Piasis, K., Nicklas, G., 1991. Late Pleistocene continental climate and oceanic variability recorded in northwest Pacific sediments. *Paleoceanography* 6 (3), 349–370. <https://doi.org/10.1029/91PA00559>.
- Huggett, R.J., 1991. *Climate, Earth Processes and Earth History*. Springer-Verlag, Berlin, 281 pp.
- Hum, L., 2002. Délkelet-dunántúli lösz–paleotalaj sorozatok keletkezésének rekonstrukciója őslénytani vizsgálatok alapján. (The reconstruction of LPS of SE Transdanubia based on paleoecological studies). *Földtani Közlemények* 13, 233–251.
- Hum, L., 2005. Középső pleisztocén tuffhorizontok megjelenése dunaszekcsői és Mórág környéki löszszelvényekben, környéki löszszelvényekben. (Middle Pleistocene tephra horizons in the profiles of Dunaszekcső and Mórág). *Malakológiai Tájékoztató* 23, 131–148.
- Hum, L., 2007. Ciklikus Klímaváltozások Kimutatása Dél-magyarországi Pleisztocén Rétegsorok Üledéktani, Geokémiai és Őslénytani Vizsgálatai Alapján. (Identification of Climatic Cycles of via Sedimentological, Geochemical, Paleontological Analyses of Transdanubian Pleistocene Sequences) OTKA Kutatási Jelentések. OTKA Research Reports.
- Hum, L., Sümeği, P., 2000. Cyclic climatic records in loess–paleosol sequences in southeastern Transdanubia (Hungary) on the basis of sedimentological,

- geochemical and malacological examination. *Geolines* 11, 99–101.
- Hum, L., Sümeği, P., 2001. Dunaszekcsői pleisztocén rétegsorok malakológiai vizsgálatai. (Malacological investigations on the Pleistocene deposits of Dunaszekcső). *Malakológiai Tájékoztató* 20, 17–27.
- Hungarian Meteorological Service: Climate Data Series 1901–2000. [http://www.met.hu/en/eghajlat/magyarorszag\\_eghajlata/eghajlati\\_adatsorok\\_1901-2000/](http://www.met.hu/en/eghajlat/magyarorszag_eghajlata/eghajlati_adatsorok_1901-2000/), last access: 20 October 2015.
- Imbrie, J., Berger, A., Boyle, E.A., Clemens, S.C., Duffy, A., Howard, W.R., Kukla, G., Kutzbach, J., Martinson, D.G., McIntyre, A., Mix, A.C., Molino, B., Morley, J.J., Peterson, L.C., Pisias, N.G., Prell, W.L., Raymo, M.E., Schackleton, N.J., Toggweiler, J.R., 1993. On the structure and origin of major glaciation cycles. 2. The 100,000-year cycle. *Paleoceanography* 8, 699–735.
- Jansen, J.H.F., Kuijpers, A., Troelstra, S.R.A., 1986. Mid-Brunhes climatic event: long-term changes in global atmosphere and ocean circulation. *Science* 232, 619–622.
- Jordanova, D., Petersen, N., 1999. Paleoclimatic record from a loess–soil profile in northeastern Bulgaria II. Correlation with global climatic events during the Pleistocene. *Geophys. J. Int.* 138, 533–540.
- Jordanova, D., Hus, J., Geeraerts, R., 2007. Palaeoclimatic implications of the magnetic record from loess/paleosol sequence Viatovo (NE Bulgaria). *Geophys. J. Int.* 171, 1036–1047.
- Jordanova, D., Hus, J., Evgoliev, J., Geeraerts, R., 2008. Paleomagnetism of the loess/paleosol sequence in Viatovo (NE Bulgaria) in the Danube Basin. *Phys. Earth Planet. Inter.* 167, 71–83.
- Joussauze, S., Taylor, K.E., 1995. Status of the Paleoclimate Modeling Intercomparison Project (PMIP). Proceedings of the First International AMIP Scientific Conference. WCRP Report, pp. 425–430.
- Jouzel, J., Masson-Delmotte, V., Cattani, O., Dreyfus, G., Falourd, S., Hoffmann, G., Minster, B., Nouet, J., Barnola, J.M., Chappellaz, J., Fischer, H., Gallet, J.C., Johnsen, S., Leuenberger, M., Loulergue, L., Luethi, D., Oerter, H., Parrenin, F., Raisbeck, G., Raynaud, D., Schilt, A., Schwander, J., Selmo, E., Souchez, R., Spahni, R., Stauffer, B., Steffensen, J.P., Stenni, B., Stocker, T.F., Tison, J.L., Werner, M., Wolff, E.W., 2007. Orbital and millennial Antarctic climate variability over the past 800,000 years. *Science* 317, 793–796.
- Juvigné, E., Horváth, E., Gábris, Gy., 1991. La Téphra de Bag: une retombée volcanique à large dispersion dans le loess pleistocène d'Europe centrale. *Eiszeitalt. Gw.* 41, 107–118.
- Kageyama, M., Briery, C., Crucifix, M., Hargreaves, J.C., Paul, A., Ramstein, G., 2012. Progress in Paleoclimate Modelling. *Climate of the Past* 9–10, Special Issue.
- Kaiser, M., Krollop, E., Scharek, P., 1998. Adatok a Duna-hordalékkúp és teraszok kapcsolatához Győr környékén. (New data Relatsh. between Danube's alluvial fan terraces Győr region.) *Földtani Közönlöny* 128 (2), 519–530.
- Kashiwaya, K., Ochiai, S., Sakai, H., Kawai, T., 2001. Orbit related long-term climate cycles revealed in a 12-My continental record from Lake Baikal. *Nature* 410, 71–74.
- Kemp, R.A., 2001. Pedogenic modification of loess: significance for paleoclimatic reconstructions. *Earth-Science Rev.* 54, 145–156.
- Klemm, W., 1969. Das Subgenus *Neostyriaca* AJ WAGNER 1920, besonders der Rassenkreis *Clausilia* (*Neostyriaca*) *corynodes* HELD 1836. *Arch. Moll* 99 (5/6), 285–311.
- Kohfeld, K.E., Harrison, S.P., 2000. How well can we simulate past climates? Evaluating the models using global palaeoenvironmental datasets. *Quat. Sci. Rev.* 19, 321–346.
- Koloszár, L., 1997. Geological Evaluation of the Udvari–2A Borehole, 1996/II. Annual Report of the Geological Institute of Hungary, pp. 149–158.
- Koloszár, L., 2003. DK-dunántúli Negyedidőszaki Képződmények Környezetföldtani Vizsgálata. (Environmental Geological Investigations of Quaternary Sequences of SE Transdanubia). PhD thesis. University of Miskolc, 70 pp. (in Hungarian).
- Koloszár, L., Lantos, M., 2001. DK-dunántúli negyedidőszaki szelvények magnetostratigráfiai korrelációja (Magnetostratigraphic correlation of the Quaternary sequences in South-eastern Transdanubia). *Földtani Közönlöny* 131, 221–231 (in Hungarian).
- Koloszár, L., Marsi, I., 1997. Stratigraphy of the Neogene and Quaternary Sequences of the Tolna Hegyhát Hills, 1996/II. Annual Report of the Geological Institute of Hungary, pp. 173–190.
- Koloszár, L., Lantos, M., Chikán, G., 2001. A Görgeteg G-1 és az Udvari U-2A fúrások negyedidőszaki képződményeinek párhuzamosítása. (Correlation of the Quaternary sediments in the Görgeteg G-1 and the Udvari U-2A boreholes). *Földtani Közönlöny* 131, 443–460 (in Hungarian).
- Koloszár, L., Marsi, I., 2010a. A Kárpát-medence legvastagabb és legteljesebb lőrszéltesora: az Udvari–2A fúrás szelvénye és kvarter rétegtani jelentősége. (The thickest and most complete loess sequence in the Carpathian Basin: the section of the borehole Udvari–2A and its significance in the Quaternary stratigraphy). *Földtani Közönlöny* 140/3, 251–262 (in Hungarian).
- Koloszár, L., Marsi, I., 2010b. The thickest and most complete loess sequence in the Carpathian Basin: the borehole Udvari–2A. *Cent. Eur. J. Geosci.* 2/2, 165–174.
- Kretzoi, M., Krollop, E., 1972. Az Alföld harmadkor végi és negyedkori rétegtana az őslénytani adatok alapján. (Late Tertiary and Quaternary stratigraphy of the Great Hungarian Plain in the light of paleontological data). *Földr. Értesítő* 21, 133–158.
- Kriván, P., Rózsavölgyi, J., 1964. Andezittuffit vezetőszint a magyarországi felsőpleisztocén (rissi) löszszelvényekből. A marker horizont adatait tartalmazó tuffit Upper-Pleistocene (Riss) loess Sect. Hungary. *Földtani Közönlöny* 94, 257–265.
- Krollop, E., 1961. A Buda Környéki Alsó-pleisztocén Mésziszapok Csiagfaunájának Állatföldrajzi És Ökológiai Vizsgálata. (Biogeographical and Ecological Analysis of Lower Pleistocene Calcareous Muds Near Buda). university doctoral dissertation. ELTE University, Budapest, 141 pp. (in Hungarian).
- Krollop, E., 1970. Őslénytani adatok a nagyalföldi pleisztocén és felső-pliocén rétegek sztratigráfijához (Paleontological data to the stratigraphy of Pleistocene and Upper Pliocene sequences of the Great Hungarian Plain). *Őslénytani Viták* 14, 5–43 (in Hungarian).
- Krollop, E., 1973. Negyedidőszaki malakológia Magyarországon. *Quaternary malacology in Hungary. Földr. Közlemények* 21, 161–171.
- Krollop, E., 1977. Middle pleistocene mollusc fauna from the Vértesszőlős Campsite of Prehistoric man. A vértesszőlősi ősemberi lelőhely középső pleisztocén Mollusca-faunája. *Földr. Közlemények* 25, 188–211.
- Krollop, E., 1981. Negyedidőszaki sztratotípusaink Molluska faunája-Süttő. (Mollusk fauna of Hungarian Pleistocene stratotypes-Süttő). *MÁFI évi jelentése* 1980-ról 371–380.
- Krollop, E., 1994. A *Neostyriaca* génusz a magyarországi pleisztocén képződményekben. (Representatives of the genus *Neostyriaca* in Hungarian Pleistocene deposits). *Malakológiai Tájékoztató* 13, 5–8.
- Krollop, E., 2003. Mollusc species of the Hungarian Pleistocene loess formations (as of Dec 31 of year 2002). *Malacol. Newsl.* 21, 13–18.
- Krollop, E., 2005. Bábaapáti Minták Malakológiai Vizsgálata (Malacological Analysis of Bábaapáti Samples). Manuscript. Hungarian Geological Institute, Budapest, Tekt, p. 1283.
- Kukla, G.J., 1977. Pleistocene land–sea correlations. *Earth-Sci. Rev.* 13, 307–374.
- Kukla, G.J., 1978. The classical European glacial stages: correlation with deep-sea sediments. *Trans. Nebr. Acad. Sci.* VI, 57–93.
- Kukla, G.J., 1987. Loess stratigraphy in central China. *Quat. Sci. Rev.* 6, 191–219.
- Kukla, G., 2005. Saalian supercycle, Mindel/Riss interglacial and Milankovitch's dating. *Quat. Sci. Rev.* 24, 1573–1583.
- Kukla, G., An, Z., 1989. Loess stratigraphy in Central China. *Palaeogeogr. Palaeoclimatol. Palaeoecol.* 72, 203–225.
- Kukla, G.J., Cilek, V., 1996. Plio-Pleistocene megacycles: record of climate and tectonics. *Palaeogeogr. Palaeoclimatol. Palaeoecol.* 120, 171–194.
- Kukla, G., Heller, F., Liu, X.M., Xu, T.C., Liu, T.S., An, Z.S., 1980. Pleistocene climates in China dated by magnetic susceptibility. *Geology* 16, 811–814.
- Laj, C., Channel, J.E.T., 2009. Geomagnetic excursions. In: Kono, M. (Ed.), *Treatise on Geophysics, Geomagnetism*. Elsevier, Amsterdam, pp. 373–416.
- Lambert, F., Bigler, M., Steffensen, J.P., Hutterli, M., Fischer, H., 2012. Centennial mineral dust variability in high-resolution ice core data from Dome C, Antarctica. *Clim. Past* 8, 609–623.
- Lang, N., Wolff, E.W., 2011. Interglacial and glacial variability from the last 800 ka in marine, ice and terrestrial archives. *Clim. Past* 7, 361–380.
- Langereis, C.G., Dekkers, M.J., De Lange, G.J., Paterne, M., Van Santvoort, P.J.M., 1997. Magnetostratigraphy and astronomical calibration of the: last 1.1 Myr from an eastern Mediterranean piston core and dating of short events in the Brunhes. *Geophys. J. Int.* 129, 75–94.
- Li, B., Li, S.-H., 2012. Luminescence dating of Chinese loess beyond 130 ka using the non-fading signal from K-feldspar. *Quat. Geochronol.* 10, 24–31.
- Lisiecki, L.M., Raymo, M.E., 2005. A Pliocene-pleistocene Stack of 57 Globally Distributed Benthic  $^{18}O$  Records, *Paleoceanography*, 20, PA1003. Data Archived at the World Data Center for Paleoclimatology, Boulder, Colorado, USA.
- Liu, T.S., Gu, X.F., An, Z.S., Fan, X.Y., 1985. *Loess and the Environment*. China Ocean Press, Beijing.
- Liu, X.M., Liu, T.S., Xu, T.C., Liu, C., Cheng, M.Y., 1987. A Preliminary study on magnetostratigraphy of a loess profile in Xifeng area, Gansu Province. In: Liu, T.S. (Ed.), *Aspects of Loess Research*. China Ocean Press, Beijing, pp. 164–174.
- Liu, X.M., Liu, T.S., Xu, T.C., Liu, C., Cheng, M.Y., 1988. The primary study on magnetostratigraphy of a loess profile in Xifeng area, Gansu Province. *Geophys. J. R. Astr. Soc.* 92, 345–348.
- Liu, X.M., Hesse, P., Rolph, T., Begét, J.E., 1999. Properties of magnetic mineralogy of Alaskan loess: evidence for pedogenesis. *Quat. Int.* 62, 93–102.
- Liu, X.M., Xia, D.S., Liu, T.S., et al., 2007. Discussion on two models of paleoclimatic records of magnetic susceptibility of Alaskan and Chinese loess (in Chinese). *Quat. Sci.* 27, 210–220.
- Liu, X.M., Liu, Z., Lü, B., Marković, S.B., Chen, J.S., Guo, H., Ma, M.M., Zhao, G.Y., Feng, H., 2012. The magnetic properties of Serbian loess and its environmental significance. *Chin. Sci. Bull.* <https://doi.org/10.1007/s11434-012-5383-9>.
- Liu, Q., Roberts, A.P., Eelco, J., Rohling, E.J., Rixiang Zhu, R., Sun, Y., 2008. Post-depositional remanent magnetization lock-in and the location of the Matuyama–Brunhes geomagnetic reversal boundary in marine and Chinese loess sequences. *Earth Plan. Sci. Lett.* 275, 102–110.
- Loulergue, L., Schilt, A., Spahni, R., Masson-Delmotte, V., Blunier, T., Lemieux, B., Barnola, J.M., Raynaud, D., Stocker, T.F., Chappellaz, J., 2008. Orbital and millennial-scale features of atmospheric CH<sub>4</sub> over the past 800 000 years. *Nature* 453, 383–386.
- Lu, H., An, Z., 1998. Palaeoclimatic significance of grain size of loess-paleosol sequence of Central China. *Sci. China Ser. D* 41, 626–631.
- Lu, H.Y., Zhang, F.Q., Liu, X.D., Robert, A., 2004. Periodicities of paleoclimatic variations recorded by loess-paleosol sequences in China. *Quat. Sci. Rev.* 23, 1891–1900.
- Lund, S.P., Williams, T., Acton, G.D., Clement, B., Okada, M., 2001. Brunhes Chron magnetic field excursions recovered from Leg 172 sediments. In: Keigwin, L.D., Rio, D., Acton, G.D., Arnold, E. (Eds.), *Proc. ODP, Sci. Results*, vol. 172, pp. 1–18.
- Lund, S., Stoner, J.S., Channell, J.E.T., Acton, G., 2006. A summary of Brunhes paleomagnetic field variability recorded in Ocean Drilling Program cores. *Phys.*

- Earth Planet. Inter., ODP Contrib. Paleomagnet. 156, 194–204.
- Lüthi, D., Le Floch, M., Bereiter, B., Blunier, T., Barnola, J.M., Siegenthaler, U., Raynaud, D., Jouzel, J., Fischer, H., Kawamura, K., Stocker, T.F., 2008. High-resolution carbon dioxide concentration record 650,000–800,000 years before present. *Nature* 453, 379–382.
- Maier, B.A., 1998. Magnetic properties of modern soils and Quaternary loessic paleosols: paleoclimatic implications. *Palaeogeogr. Palaeoclimatol. 137*, 25–54.
- Marković, S.B., Oches, E., Sumegi, P., Jovanović, M., Gaudenyi, T., 2006. An introduction to the upper and middle pleistocene loess-paleosol sequences of Ruma section (Vojvodina, Serbia). *Quat. Int.* 149, 80–86.
- Marković, S.B., Bokhorst, M., Vandenbergh, J., Oches, E.A., Zoller, L., McCoy, W.D., Gaudenyi, T., Jovanović, M., Hambach, U., Machalet, B., 2008. Late pleistocene loess-paleosol sequences in the Vojvodina region, north Serbia. *J. Quat. Sci.* 23, 73–84.
- Marković, S.B., Hambach, U., Catto, N., Jovanović, M., Buggle, B., Machalet, B., Zoller, L., Glaser, B., Frechen, M., 2009. The middle and late Pleistocene loess-paleosol sequences at Batajanica, Vojvodina, Serbia. *Quat. Int.* 198, 255–266.
- Marković, S.B., Hambach, U., Stevens, T., Kukla, G.J., Heller, F., McCoy, W.D., Oches, E.A., Buggle, B., Zoller, L., 2011. The last million years recorded at the Stari Slankamen (Northern Serbia) loess-paleosol sequence: revised chronostratigraphy and long-term environmental trends. *Quat. Sci. Rev.* 30, 1142–1154.
- Marković, S., Hambach, U., Stevens, T., Jovanović, M., O'Hara-Dhand, K., Basarin, B., Lu, H., Smalley, I., Buggle, B., Zech, M., Svirčev, Z., Sümeği, P., Milojković, N., Zoller, L., 2012a. Loess in the Vojvodina region (northern Serbia): an essential link between European and Asian pleistocene environments. *Neth. J. Geosci. Geol. Mijnb.* 91, 173–188.
- Marković, S.B., Hambach, U., Stevens, T., Basarin, B., O'Hara-Dhand, K., Gavrilov, M., Gavrilov, M., Smalley, I., Teofanov, N., 2012b. Relating the astronomical time-scale to the loess-paleosol sequences in Vojvodina, Northern Serbia. In: Berger, A., Mesinger, F., Sijacki, D. (Eds.), *Climate Change: Inferences from Paleoclimate and Regional Aspects*. Springer-Verlag, Vienna, pp. 65–78.
- Marković, S.B., Stevens, T., Kukla, G.J., Hambach, U., Fitzsimmons, K.E., Gibbard, P., Buggle, B., Zech, M., Guo, Z., Hao, Q., Wu, H., O'Hara Dhand, K., Smalley, I.J., Újvári, G., Sümeği, P., Timar-Gabor, A., Veres, D., Sirocko, F., Vasiljevic, D.A., Jary, Z., Svensson, A., Jovic, V., Lehmkühl, F., Kovács, J., Svirčev, Z., 2015. Danube loess stratigraphy - towards a pan-European loess stratigraphic model. *Earth-Sci. Rev.* 148, 228–258.
- Marsi, I., Gy, Don, Földvári, M., Kolozsár, L., Kovács-Pálffy, P., Krolopp, E., Lantos, M., Nagy-Bodor, E., Zilahi-Sebess, L., 2004. Quaternary sediments of the north-eastern Mórág Block. *Ann. Rep. Geol. Inst. Hung.* 2003, 343–360.
- Márton, P., 1979. Paleomagnetism of the Paks brickyard exposures. *Acta Geol. Hung.* 22, 443–449.
- Márton, P., 1998. Report of the Results of Paleomagnetic Measurements of Boreholes Udvari (U-2a) and Diósberény (Db-ia). Manuscript. Hungarian Geological Institute (in Hungarian).
- Matasova, G., Petrovsky, E., Jordanova, N., et al., 2001. Magnetic study of Late Pleistocene loess/paleosol sections from Siberia: palaeoenvironmental implications. *Geophys. J. Int.* 147, 367–380.
- McManus, J.F., Oppo, D.W., Cullen, J.L., 1999. A 0.5-million-year record of millennial-scale climate variability in the North Atlantic. *Science* 283, 971–975.
- Michalk, D.M., Böhnel, H.N., Nowaczyk, N.R., Augíre-Díaz, G.J., López-Martínez, M., Ownby, S., Negendank, J.F.W., 2013. Evidence for geomagnetic excursions recorded in Brunhes and Matuyama Chron lavas from the trans-Mexican volcanic belt. *J. Geophys. Res. Solid Earth* 118, 2648–2669.
- Murray, A.S., Schmidt, E.D., Stevens, T., Buylaert, J.P., Marković, S.B., Tsukamoto, S., Frechen, M., 2014. Dating Middle Pleistocene loess from Stari Slankamen (Vojvodina, Serbia) — limitations imposed by the saturation behaviour of an elevated temperature IRSL signal. *Catena* 117, 34–42.
- Neftel, A., Oeschger, H., Staffelbach, T., Stauffer, B., 1988. CO<sub>2</sub> Record in the Byrd ice core 50,000–5000 years BP. *Nature* 331, 609–611.
- Novothy, Á., Frechen, M., Horváth, E., Bradák, B., Oches, E.A., McCoy, W.D., Stevens, T., 2009. Luminescence and amino acid racemization chronology of the loess paleosol sequence at Süttő. *Hung. Quat. Int.* 198, 62–76.
- Nowaczyk, N.R., Frederichs, T.W., 1999. Geomagnetic events and relative paleointensity variations during the past 300 ka as recorded in Kolbeinsey Ridge Sediments, Iceland Sea: indication for a strongly variable geomagnetic field. *Int. J. Earth Sci.* 88, 116–131.
- Nowaczyk, N.R., Knies, J., 2000. Magnetostratigraphic results from Eastern Arctic Ocean—AMS14C ages and relative paleointensity data of the Mono Lake and Laschamp geomagnetic events. *Geophys. J. Int.* 140, 185–197.
- Nutgeren, C., Vandenbergh, J., Huissleden, J.K., van, An, Z., 2004. A Quaternary climate record based on grain-size analysis from the Luochuan loess section on the central loess plateau, China. *Glob. Plan. Change* 41, 167–183.
- Obrecht, I., Zeeden, C., Hambach, U., Veres, D., Markovic, S.B., Böskén, J., Svirčev, Z., Bacevic, N., Gavrilov, M.B., Lehmkühl, F., 2016. Tracing the influence of Mediterranean climate on Southeastern Europe during the past 350,000 years. *Nat. Sci. Rep.* 6 <https://doi.org/10.1038/srep36334>, 36334.
- Oches, E.A., McCoy, W., 1995a. Amino acid geochronology applied to the correlation and dating of central European loess deposits. *Quat. Sci. Rev.* 14, 767–782.
- Oches, E.A., McCoy, W.D., 1995b. Aminostratigraphic evaluation of conflicting age estimates for the “Young Loess” of Hungary. *Quat. Res.* 44, 160–170.
- Oches, E.A., McCoy, W., 2001. Historical developments and recent advances in amino acid geochronology applied to loess research: examples from North America, Europe and China. *Earth Sci. Rev.* 54, 173–192.
- Panaiotu, C.G., Panaiotu, C.E., Grama, A., Necula, C., 2001. Paleoclimatic record from a loess-paleosol profile in southeastern Romania. *Phys. Chem. Earth A* 26, 893–898.
- Parrenin, F., Barnola, J.M., Beer, J., Blunier, T., Castellano, E., Chappellaz, J., Dreyfus, G., Fischer, H., Fujita, S., Jouzel, J., Kawamura, K., Lemieux-Dudon, B., Loulergue, L., Masson-Delmotte, V., Narcisi, B., Petit, J.-R., Raisbeck, G., Raynaud, D., Ruth, U., Schwander, J., Severi, M., Spahni, R., Steffensen, J.P., Svensson, A., Udisti, R., Waelbroeck, C., Wolff, E., 2007. The EDC3 chronology for the EPICA Dome C ice core. *Clim. Past* 3, 485–497. <https://doi.org/10.5194/cp-3-485-2007>.
- Pazonyi, P., Kordos, L., Magyari, E., Marinova, E., Füköh, L., Venczel, M., 2014. Pleistocene vertebrate faunas of the Süttő travertine complex (Hungary). *Quat. Int.* 319, 50–63.
- Pécsi, M., 1975. A magyarországi lösz szelvények litosztratiográfiai tagolása (Lithostratigraphical subdivision of Hungarian loess profiles). *Földr. Közlemények* 23, 217–230 (in Hungarian).
- Pécsi, M., 1979. Lithostratigraphical subdivision of the loess profiles at Paks. *Acta Geol. Hung.* 22, 409–418.
- Pécsi, M., 1990. Loess is not just the accumulation of dust. *Quat. Int.* 7–8, 1–21.
- Pécsi, M., 1993. *Negyedkor És Löszkutatás*. (Quaternary and Loess Research). Akadémiai Kiadó, Budapest, Hungary, 375p. (in Hungarian).
- Pécsi, M., 1995. Loess stratigraphy and Quaternary climatic change. In: Pécsi, M., Schweitzer, F. (Eds.), *Concept of Loess, Loess-paleosol Stratigraphy*. Loess in Form, vol. 3, pp. 23–30.
- Pécsi, M., Pevzner, M.A., 1974. Paleomagnetic measurements in the loess sequences at Paks and Dunaföldvár. *Hung. Földr. Közlemények* 22, 215–219.
- Pécsi, M., Schweitzer, F., 1993. Long-term terrestrial records of the middle Danubian Basin. *Quat. Int.* 17, 5–14.
- Pécsi, M., Schweitzer, F., Balogh, J., Balogh, M., Havas, J., Heller, F., 1995. A new loess paleosol lithostratigraphical sequence at Paks (Hungary). *Loess Form* 3, 63–78.
- Pigati, J.S., Quade, J., Shanahan, T.M., Haynes Jr., C.V., 2004. Radiocarbon dating of minute gastropods and new constraints on the timing of spring-discharge deposits in southern Arizona, USA. *Palaeogeogr. Palaeoclimatol. Palaeoecol.* 204, 33–45.
- Pigati, J.S., Rech, J.A., Nekola, J.C., 2010. Radiocarbon dating of small terrestrial gastropod shells in North America. *Quat. Geochron.* 5, 519–532.
- Pigati, J.S., McGehehin, J.P., Muhs, D.R., Bettis III, E.A., 2013. Radiocarbon dating late Quaternary loess deposits using small terrestrial gastropod shells. *Quat. Sci. Rev.* 76, 114–128.
- Poulet, A., Horvath, E., Gabris, G., Juvigné, E., 1999. The Bag tephra, a widespread tephrochronological marker in Middle Europe: chemical and mineralogical investigations. *Bull. Volcanol.* 60, 265–272.
- Porter, S.C., 2001. Chinese loess record of monsoon climate during the last glacial–interglacial cycle. *Earth-Sci. Rev.* 54, 115–128. [https://doi.org/10.1016/S0012-8252\(01\)00043-5](https://doi.org/10.1016/S0012-8252(01)00043-5).
- Porter, S.C., 2007. Loess records—China. In: Scott, A.E. (Ed.), *Encyclopedia of Quaternary Science*. Elsevier, Oxford, pp. 1429–1440. <https://doi.org/10.1016/B0-44-452747-8/00160-5>.
- Prokopenko, A.A., Karabanov, E.B., Williams, D.F., Kuzmin, M.I., Shackleton, N.J., Crowhurst, S., Peck, J.A., Gvozdkov, A.N., King, J.W., 2001. Biogenic silica record of the Lake Baikal response to climate forcing during the Brunhes. *Quat. Res.* 55, 123–132.
- Prokopenko, A.A., Williams, D.F., Kuzmin, M.I., Karabanov, E.B., Khurshovich, G.K., Peck, J.A., 2002. Muted climate variations in continental Siberia during the mid-Pleistocene epoch. *Nature* 418, 65–68.
- Pye, K., 1995. Nature, origin and accumulation of loess. *Quat. Sci. Rev.* 14, 653–667.
- Rădan, S.C., 2012. Towards a historical synopsis of dating the loess from the Romanian Plain and Dobrogea: authors and methods through time. *GeoEcoMar* 18, 153–172.
- Rapp, D., 2012. *Glacials and Interglacials: Measurement, Interpretation and Models*. Springer-Verlag, Berlin. <https://doi.org/10.1007/9783-642-30029-5-11>.
- Raymo, M.E., Lisiecki, L.E., Nisancioglu, K.H., 2006. Plio-Pleistocene ice volume, Antarctic climate, and the global  $\delta^{18}O$  record. *Science* 313, 492–495.
- Razi Rad, M., 1976. *Schwermineraluntersuchungen zur Quartärstratigraphie am Mittelrhein*, vol. 28. Sonderveröffentlichungen des Geologischen Instituts der Universität Köln, 164 pp.
- Reimer, P.J., Bard, E., Bayliss, A., Warren Beck, J., Blackwell, P.G., Bronk Ramsey, Ch., Grootes, P.M., Guilderson, T.P., Hafflidason, H., Hajdas, I., Hatt, e, Ch, Heaton, T.J., Hoffmann, D.L., Hogg, A.G., Hughen, K.A., Kaiser, K.F., Kromer, B., Manning, S.W., Niu, M., Reimer, R.W., Richards, D.A., Scott, E.M., Southon, J.R., Staff, R.A., Turney, Ch.S.M., van der Plicht, J., 2013. IntCal13 and Marine13 radiocarbon age calibration curves 0–50,000 years cal BP. *Radiocarbon* 55, 1869–1887.
- Richmond, G.M., 1996. The INQUA-approved provisional Lower/Middle Pleistocene boundary. In: Turner, C. (Ed.), *The Early–middle Pleistocene in Europe*. Balkema, Rotterdam, pp. 319–327.
- Roberts, H.M., 2012. Testing Post-IR IRSL protocols for minimising fading in feldspars, using Alaskan loess with independent chronological control. *Radiat. Meas.* 47, 716–724.
- Sági, T., Kiss, B., Bradák, B., Harangi, Sz., 2008. Középső-pleisztocén löszben előforduló vulkáni képződmények Magyarországon: terepi és petrográfiai jellemzők (Middle Pleistocene volcanic deposits in loess in Hungary: field and petrographical characteristics). *Földtani Közlemények* 138, 297–310.
- Sartori, M., Heller, F., Forster, T., Borkovec, M., Hammann, J., Vincent, E., 1999.

- Magnetic properties of loess grain size fractions from the section at Paks (Hungary). *Phys. Earth Plan. Inter* 116, 53–64.
- Sartori, M., 2000. The Quaternary Climate in Loess Sediments: Evidence from Rock and mineral Magnetic and Geochemical Analysis. PhD dissertation. ETH-Zurich, Switzerland, 238p.
- Schmidt, E.D., Tsukamoto, S., Frechen, M., Murray, A.S., 2014. Elevated temperature IRSL dating of loess sections in the East Eifel region of Germany. *Quat. Int.* 334–335, 141–154.
- Singer, B.S., 2007. Polarity transitions: radioscopic dating. In: Gubbins, D., Herrero-Bervera, B. (Eds.), *Encyclopedia of Geomagnetism and Paleomagnetism*. Springer, Dordrecht, The Netherlands, pp. 834–839.
- Singer, B.S., 2014. A Quaternary geomagnetic instability time scale. *Quat. Geochron* 21, 29–52.
- Singer, B.S., Relle, M.K., Hoffmann, K.A., Battle, A., Laj, C., Guillou, H., Carracedo, J.C., 2002. Ar/Ar ages from transitionally magnetized lavas on La Palma, Canary Islands, and the geomagnetic instability timescale. *J. Geophys. Res.* 107 (B11), 2307. <https://doi.org/10.1029/2001JB001613>.
- Singer, B.S., Jicha, B.R., Kirby, B.T., Geissman, J.W., Herrero-Bervera, E., 2008a. 40Ar/39Ar dating links Albuquerque Volcanoes to the Pringle Falls excursion and the geomagnetic instability time scale. *Earth Plan. Sci. Lett.* 267, 584–595.
- Singer, B.S., Hoffmann, K., Schnepf, E., Guillou, H., 2008b. Multiple Brunhes Chron excursions recorded in West Eifel (Germany) volcanics: support for long-held mantle control over the non-axial dipole field. *Phys. Planet. Int.* 169, 28–40.
- Singer, B.S., Guillou, H., Jicha, B.R., Zanella, E., Camps, P., 2014. Refining the quaternary geomagnetic instability timescale (GITS): lava flow recordings of the Blake and post-blake excursions. *Quat. Geochron* 21, 16–28.
- Singhvi, A.K., Bronger, A., Pant, R.K., Sauer, W., 1987. Thermoluminescence dating and its implications for the chrono-stratigraphy of loess-paleosol sequences in the Kashmir valley (India). *Chem. Geol.* 65, 45–56.
- Song, Y.G., Shi, Z.T., Fang, X.M., et al., 2010. Loess magnetic properties in the Ili Basin and their correlation with the Chinese Loess Plateau. *Sci. China. Ser. D-Earth Sci.* 53, 419–431.
- Suangwen, Y., Huayu, L., Stevens, T., 2012. SAR TT-OSL dating of loess deposits in the Horqin dunefield (northeastern China). *Quat. Geochron* 10, 56–61.
- Sun, Y.B., Clemens, S.C., An, Z.S., Yu, Z.W., 2006. Astronomical timescale and palaeoclimatic implication of stacked 3.6-Myr monsoon records from the Chinese Loess Plateau. *Quat. Sci. Rev.* 25, 33–48.
- Sun, Y., Chen, T., Xie, Q., 2009. Magnetic susceptibility of the Xifeng section and its climatic significance. *Chin. J. Geochem* 28, 81–85.
- Sümeği, P., 1991. Jelentés Az 1991-ben a Basaharci Löszfeltáráson Elvégzett Quartermalakológiai Kutatásokról (Report on quartermalakological investigations on samples from the loess of Basaharc in the year of 1991) – Geographical Research Institute of the HAS, Budapest and Department of Mineralogy and Geology, Kossuth University, Debrecen, pp. 1–120.
- Sümeği, P., 2007. Magyarország Negyedidőszak Végi Környezettörténete. (Environmental History of Hungary for the Younger - Quarter). Academic doctoral dissertation. HAS, Budapest – Szeged, 428p.
- Sümeği, P., Hertelendi, E., 1998. Reconstruction of microenvironmental changes in the Kopasz Hill loess area at Tokaj (Hungary) between 15 and 70 ka BP. *Radiocarbon* 40, 855–863.
- Sümeği, P., Krolopp, E., 2005. A basaharci téglagyári szelvény rétegtani és paleo-ökológiai vizsgálata. (Results of stratigraphic and paleoecological investigations of the loess/paleosol sequence of Basaharc brickyard). *Földtani Közönlöny* 135, 209–232.
- Sümeği, P., Krolopp, E., 2006. A basaharci téglagyári löszfeltárási Mollusca-faunája. (Mollusk fauna of the Basaharc brickyard). *Malakológiai Tájékoztató* 24, 15–30.
- Sümeği, P., Gulyás, S., 2009. The Evolution of the Loess Mollusk Fauna of the Carpathian Basin, Loessfest09, Novi Sad. Book of Abstracts.
- Sümeği, P., Krolopp, E., Rudner, E., 2002. Negyedidőszak végi ökoszisztémái változások térben és időben a Kárpát-medencében. (Environmental changes in space and time during the late Quaternary of the Carpathian Basin). *Földtani Közönlöny* 132, 5–22.
- Sümeği, P., Molnár, M., Svingor, É., Szántó, Zs, Hum, L., Gulyás, S., 2007. The results of radiocarbon analysis of Upper Weichselian loess sequences from Hungary. *Radiocarbon* 49, 1023–1028.
- Sümeği, P., Gulyás, S., Persaits, G., Páll, D.G., Molnár, D., 2011a. The loess-paleosol sequence of Basaharc (Hungary) revisited: mollusc-based paleoecological results for the Middle and Upper Pleistocene. *Quat. Int.* 240, 181–192.
- Sümeği, P., Gulyás, S., Persaits, G., 2011b. Multiproxy paleoenvironmental analysis of long-term climatic fluctuations in Southwest Hungary reading terrestrial archives. XVIII. INQUA Congress, Bern, Switzerland. *Quat. Int.* 279–280, 477.
- Sümeği, P., Persaits, G., Gulyás, S., 2012a. Woodland-grassland Ecotonal Shifts in Environmental Mosaics: Lessons learnt from the environmental history of the Carpathian Basin (Central Europe) during the Holocene and the last ice age based on investigation of paleobotanical and mollusk remains. In: Myster, R.W. (Ed.), *Ecotones between forest and Grassland*. Springer-Verlag, New York, pp. 13–37.
- Sümeği, P., Gulyás, S., Persaits, G., Szelepcsényi, Z., 2012b. Long environmental change in the forest steppe habitat of the Great Hungarian Plains based on paleoecological data. In: Rakonczai, J., Ladányi, Zs (Eds.), *Review of Climate Change Research Programme at the University of Szeged (2010-2012)*. Institute of Geography and Geology, University of Szeged, Szeged, pp. 7–24.
- Sümeği, P., Náfrádi, K., Molnár, D., Sávia, Sz., 2015. Results of paleoecological studies in the loess region of Szeged-Óhalom (SE Hungary). *Quat. Int.* 372, 66–78.
- Tegen, I., Laci, A.A., 1996. Modeling of particle size distribution and its influence on the radiative properties of mineral dust aerosol. *J. Geophys. Res.* 101, 19237–19244.
- Terhorst, B., Kühn, P., Damm, B., Hambach, U., Meyer-Heintze, S., Sedov, S., 2014. Paleoenvironmental fluctuations as recorded in the loess-paleosol sequence of the Upper Paleolithic site Krems-Wachtberg. *Quat. Int.* 351, 67–82.
- Thiel, C., Buylaert, J.P., Murray, A.S., Terhorst, B., Hofer, I., Tsukamoto, S., Frechen, M., 2011. Luminescence dating of the Stratzing loess profile (Austria) – testing the potential of an elevated temperature post-IR IRSL protocol. *Quat. Int.* 234, 23–31.
- Thiel, C., Horváth, E., Frechen, M., 2014. Revisiting the loess/paleosol sequence of Paks in Hungary: a post-IR IRSL-based chronology for the „Young Loess Series”. *Quat. Int.* 319, 88–98.
- Tzedakis, P.C., Hooghiemstra, H., Pali, H., 2006. The last 1.35 million years at Tenaghi Philippon: revised chronostratigraphy and long-term vegetation trends. *Quat. Sci. Rev.* 25, 3416–3430.
- USDA Soil Survey Staff, 1992. Keys to Soil Taxonomy. United States Department of Agriculture, Soil Conservation Service, Soil Management Support Services Technical Monograph No. 19, fifth ed. Pocahontas Press, Blacksburg, VA.
- Újvári, G., Kovács, J., Varga, Gy, Raucsik, B., Marković, S.B., 2010. Dust flux estimates for the Last Glacial Period in East Central Europe based on terrestrial records of loess deposits: a review. *Quat. Sci. Rev.* 29, 3157–3166.
- Újvári, G., Varga, A., Raucsik, B., Kovács, J., 2014a. The Paks loess-paleosol sequence: a record of chemical weathering and provenance for the last 800 ka in the mid-Carpathian Basin. *Quat. Int.* 319, 22–37.
- Újvári, G., Molnár, M., Novothny, Á., Páll-Gergely, B., Kovács, J., Várhegyi, A., 2014b. AMS 14C and OSL/IRSL dating of the Dunaszekcső loess sequence (Hungary): chronology for 20 to 150 ka and implications for establishing reliable age-depth models for the last 40 ka. *Quat. Sci. Rev.* 106, 140–154.
- Vandenbergh, J., 2000. A global perspective of the European chronostratigraphy for the past 650 ka. *Quat. Sci. Rev.* 19, 1701–1707.
- Van den Boogaard, P., Schminke, H.-U., 1990. Die Entwicklungsgeschichte des Mittelrheinraumes und die Eruptionsgeschichte des Osteifel-Vulkanfeldes. In: Schirmer, W. (Ed.), *Rheingeschichte zwischen Mosel und Maas*. Deutscher Fachschriften-Verlag, Wiesbaden, pp. 166–190.
- Varga, Gy., 2011. Similarities among the Plio-Pleistocene terrestrial aeolian dust deposits in the world and in Hungary. *Quat. Int.* 234, 98–108.
- Varga, Gy., 2012. Az eolikus por mennyiségének változásai a Kárpát-medencében a pliocén-től napjainkig a globális folyamatok tükrében. PhD thesis. University of Pécs, 112 pp.
- Varga, A., Újvári, G., Raucsik, B., 2011. Tectonic versus climatic control on the evolution of a loess-paleosol sequence at Beremend, Hungary: an integrated approach based on paleoecological, clay mineralogical, and geochemical data. *Quat. Int.* 240, 71–86.
- Vasiliniuc, S., Vandenbergh, D.A.G., Timar-Gabor, A., Panaiotu, C., Cosma, C., Van den haute, P., 2012. Testing the potential of elevated temperature post-IR-IRSL signals for dating Romanian loess. *Quat. Geochron.* 10, 75–80.
- Wacha, L., Frechen, M., 2011. The geochronology of the Gorjanović loess section in Vukovar, Croatia. *Quat. Int.* 240, 87–99.
- Wacha, L., Galović, L., Koloszar, L., Magyar, Á., Chikán, G., Marsi, I., 2013. The chronology of the Saregrad II loess-paleosol section (Eastern Croatia). *Geol. Croat.* 66 (3), 191–203.
- Wake, B., 2013. Reconstructing temperature. *Nat. Clim. Change* 3, 15. <https://doi.org/10.1038/nclimate1800>.
- Williams, D.F., Peck, J., Karabanov, E.B., Prokopenko, A.A., Kravchinsky, V., King, J., Kuzmin, M.I., 1997. Lake Baikal record of continental climate response to orbital insolation during the past 5 million years. *Science* 278, 1114–1117.
- Wintle, A.G., Packman, S.C., 1988. Thermoluminescence ages for three sections in Hungary. *Quat. Sci. Rev.* 7, 315–320.
- Wu, B., Wu, N.Q., 2011. Terrestrial mollusc records from Xifeng and Luochuan L9 loess strata and their implications for paleoclimatic evolution in the Chinese Loess Plateau during marine Oxygen Isotope Stages 24–22. *Clim. Past* 7, 349–359.
- Xu, B., Gu, Z., Han, J., Hao, Q., Lu, Y., Wang, L., Wu, N., Peng, Y., 2011. Radiocarbon age anomalies of land snail shells in the Chinese Loess Plateau. *Quat. Geochron.* 6, 383–389.
- Yin, Q.Z., 2013. Insolation-induced mid-Brunhes transition in Southern Ocean ventilation and deep ocean temperature. *Nature* 494, 222–225.
- Yin, Q.Z., Berger, A., 2012. Individual contribution of insolation and CO<sub>2</sub> to the interglacial climates of the past 800,000 years. *Clim. Dyn.* 38, 709–724.
- Yin, Q.Z., Guo, Z.T., 2006. Mid-Pleistocene vermiculated red soils in southern China as an indication of unusually strengthened East Asian monsoon. *Chin. Sci. Bull.* 51 (2), 213–220.
- Yin, Q.Z., Guo, Z.T., 2008. Strong summer monsoon during the cool MIS-13. *Clim. Past* 4, 29–34.
- Yin, Q.Z., Berger, A., Driesschaert, E., Gooze, H., Loutre, M.F., Crucifix, M., 2008. The Eurasian ice sheet reinforces the East Asian summer monsoon during the interglacial 500,000 years ago. *Clim. Past* 4, 79–90.
- Zagwijn, W., 1985. An outline of the Quaternary stratigraphy of The Netherlands. *Geol. Mijnb.* 64, 17–24.

- Zagwijn, W., 1996. The Cromerian complex stage of The Netherlands and correlation with other areas in Europe. In: Turner, C. (Ed.), *The Early Middle Pleistocene in Europe*. Balkema, Rotterdam, pp. 145–172.
- Zhang, W., Zhen, J., Li, G., 2015. Shifting material source of Chinese loess since ~ 2.7 Ma reflected by Sr isotopic composition. *Nat. Sci. Rep.* 5, 10235. <https://doi.org/10.1038/srep10235>.
- Zhou, L.P., Oldfield, F., Wintle, A.G., Robinson, S.G., Wang, J.T., 1990. Partly pedogenic origin of magnetic variations in Chinese loess. *Nature* 346, 737–739.
- Zhou, L.P., Shackleton, N.J., 1999. Misleading positions of geomagnetic reversal boundaries in Eurasian loess and implications for correlation between continental and marine sedimentary sequences. *Earth Plan. Sci. Lett.* 168, 117–130.
- Zhou, W.J., Beck, W., Kong, X.H., An, Z.S., Qiang, X.K., Wu, Z.K., Xian, F., Ao, H., 2014. Timing of the Brunhes-Matuyama magnetic polarity reversal in Chinese loess using  $^{10}\text{Be}$ . *Geology* 42, 467–470.
- Zöller, L., Wagner, G.A., 1990. Thermoluminescence dating of loess—recent developments. *Quat. Int.* 7/8, 119–128.